Symmetries of PQ Patterns

Polyline fairness is a popular choice for a regularizer for planar-quadrilateral meshes in the literature. The objective is to straighten the polylines by minimizing second-order differences between neighboring vertices on a polyline, and this is equivalent to applying symmetries with respect to vertices. However, this fairness measure is restrictive in the sense that it is only applicable to meshes that are aligned with conjugate directions on the reference surface. Our computation with edge-midpoint symmetries introduces more degrees of freedom and is less sensitive to the initial alignment.

In the following, we explain why the edge-midpoint symmetry regularizer is more flexible than the polyline fairness regularizer. We consider quadrilateral patterns, $\mathbf{p}_{i,j}$, $i, j \in \mathbb{Z}$, on the (x, y)-plane, which are liftable to a paraboloid, S, while maintaining face planarity. We define S as $z = \kappa_1 x^2 + \kappa_2 y^2$, $\kappa_1\kappa_2 \neq 0$. Following the Appendix, we consider the induced quadratic form $\langle \mathbf{a}, \mathbf{b} \rangle := \kappa_1 x_a x_b + \kappa_2 y_a y_b$ on the (x, y)-plane, the squared norm $|\mathbf{a}|^2 = \langle \mathbf{a}, \mathbf{a} \rangle$, and the conjugacy relation $\langle \mathbf{a}, \mathbf{b} \rangle = 0$.

Polyline fairness Straight polylines hold:

$$\begin{aligned} \frac{1}{2}(\mathbf{p}_{i+1,j} + \mathbf{p}_{i-1,j}) &= \mathbf{p}_{i,j}, \\ \frac{1}{2}(\mathbf{p}_{i,j+1} + \mathbf{p}_{i,j-1}) &= \mathbf{p}_{i,j}. \end{aligned} \tag{1}$$

These conditions are essentially symmetries with respect to vertices. An equivalent formulation is:

$$\begin{aligned} \mathbf{p}_{i+1,j} - \mathbf{p}_{i,j} &\equiv \mathbf{u}, \\ \mathbf{p}_{i,j+1} - \mathbf{p}_{i,j} &\equiv \mathbf{v}, \end{aligned} \tag{2}$$

where $\mathbf{u}, \mathbf{v} \in \mathbb{R}^2$ are the respective edge vectors. With perfect straight polylines of equally distributed vertices, the quadrilaterals of the tiling are congruent parallelograms that are translations of each other. When $\mathbf{u}$, $\mathbf{v}$ and a single vertex are given, the whole pattern is fixed.

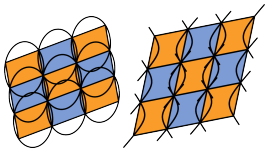

Figure 1: *Polyline fairness requires a quad mesh to be initialized according to conjugate directions.*

To be liftable to a paraboloid while maintaining planarity, every parallelogram must be inscribed to a conic in the form of $|\mathbf{p} - \mathbf{c}|^2 = \gamma$, $\gamma \in \mathbb{R}$, as shown in the Appendix. This requires $\mathbf{u}$ and $\mathbf{v}$ to be conjugate: $\langle \mathbf{u}, \mathbf{v} \rangle = 0$.

For the hyperbolic case, $\kappa_1\kappa_2 < 0$, the asymptotic directions $\mathbf{d} := \lambda(\sqrt{\kappa_2}, \pm\sqrt{\kappa_1})$ are self-conjugate, as $\langle \mathbf{d}, \mathbf{d} \rangle = \kappa_1 x_\mathbf{d} x_\mathbf{d} + \kappa_2 y_\mathbf{d} y_\mathbf{d} = \kappa_1|\kappa_2| + \kappa_2|\kappa_1| = 0$. When one family of polylines is aligned in a direction close to an asymptotic direction, the other family of polylines must also be aligned with a close direction, which results in ill-shaped narrow quads. From this, we determine that the polyline fairness is only effective for conjugate directions that are close to orthogonal, i.e., principal directions, and are far from asymptotes, (see Figure 1).

Edge midpoint symmetry Symmetries with respect to edge midpoints require each pair of adjacent faces to be symmetric with respect to the midpoint of their common edge:

$$\begin{aligned} \frac{1}{2}(\mathbf{p}_{i\pm1,j} + \mathbf{p}_{i\mp1,j+1}) &= \frac{1}{2}(\mathbf{p}_{i,j} + \mathbf{p}_{i,j+1}), \\ \frac{1}{2}(\mathbf{p}_{i,j\pm1} + \mathbf{p}_{i+1,j\mp1}) &= \frac{1}{2}(\mathbf{p}_{i,j} + \mathbf{p}_{i+1,j}). \end{aligned} \tag{3}$$

By linear combinations, those conditions are equivalent to:

$$\begin{aligned} \mathbf{p}_{i+1,j+1} - \mathbf{p}_{i,j} &\equiv \mathbf{s}, \\ \mathbf{p}_{i+1,j-1} - \mathbf{p}_{i,j} &\equiv \mathbf{t}, \end{aligned} \tag{4}$$

where $\mathbf{s}, \mathbf{t} \in \mathbb{R}^2$ are the diagonal vectors of every quad in the mesh. This produces two more degrees of freedom for quad tilings in comparison with polyline fairness, since the actual positions of the diagonals can vary and the quad is not constrained to be a parallelogram anymore (see Figure 2). Effectively, the quadrilateral pattern is naturally decomposed to two independent sets of vertices. These degrees of freedom are apparent on computed results with general surfaces as well (see Figure 3).

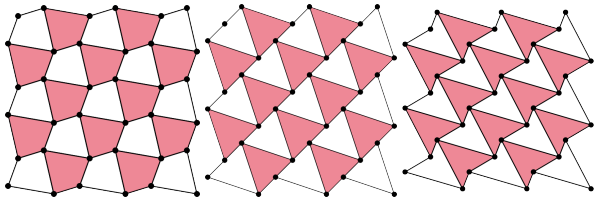

Figure 2: *Imposing edge-midpoint symmetries introduces two more degrees of freedom in comparison with polyline fairness.*

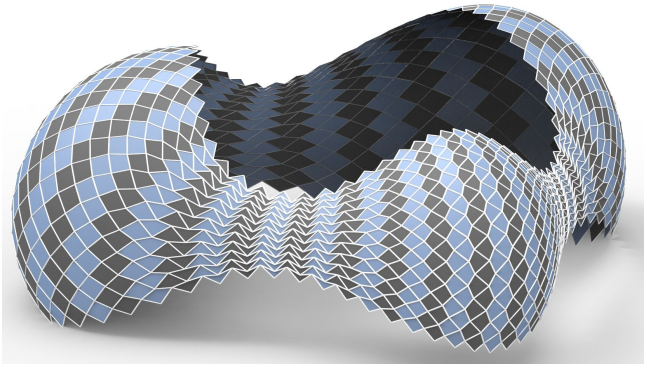

Figure 3: *A PQ mesh on the wave model optimized with edge-midpoint regularizers. The initial pattern is not aligned with conjugate directions.*

Additional Figures

In the following we show several additional results and an example of future work.

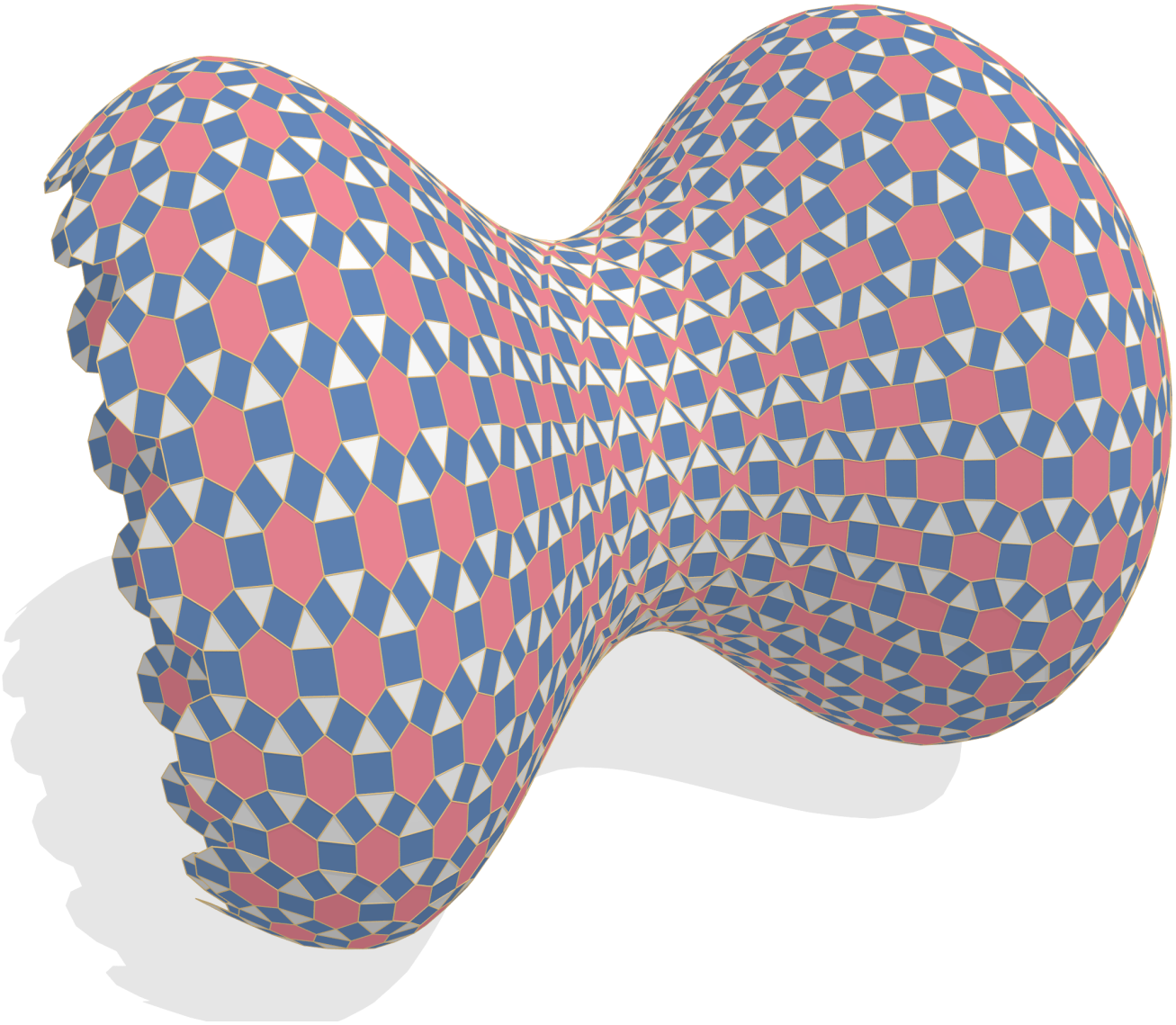

Figure 4: *A* $(3, 4, 6, 4)$ *pattern using face symmetries.*

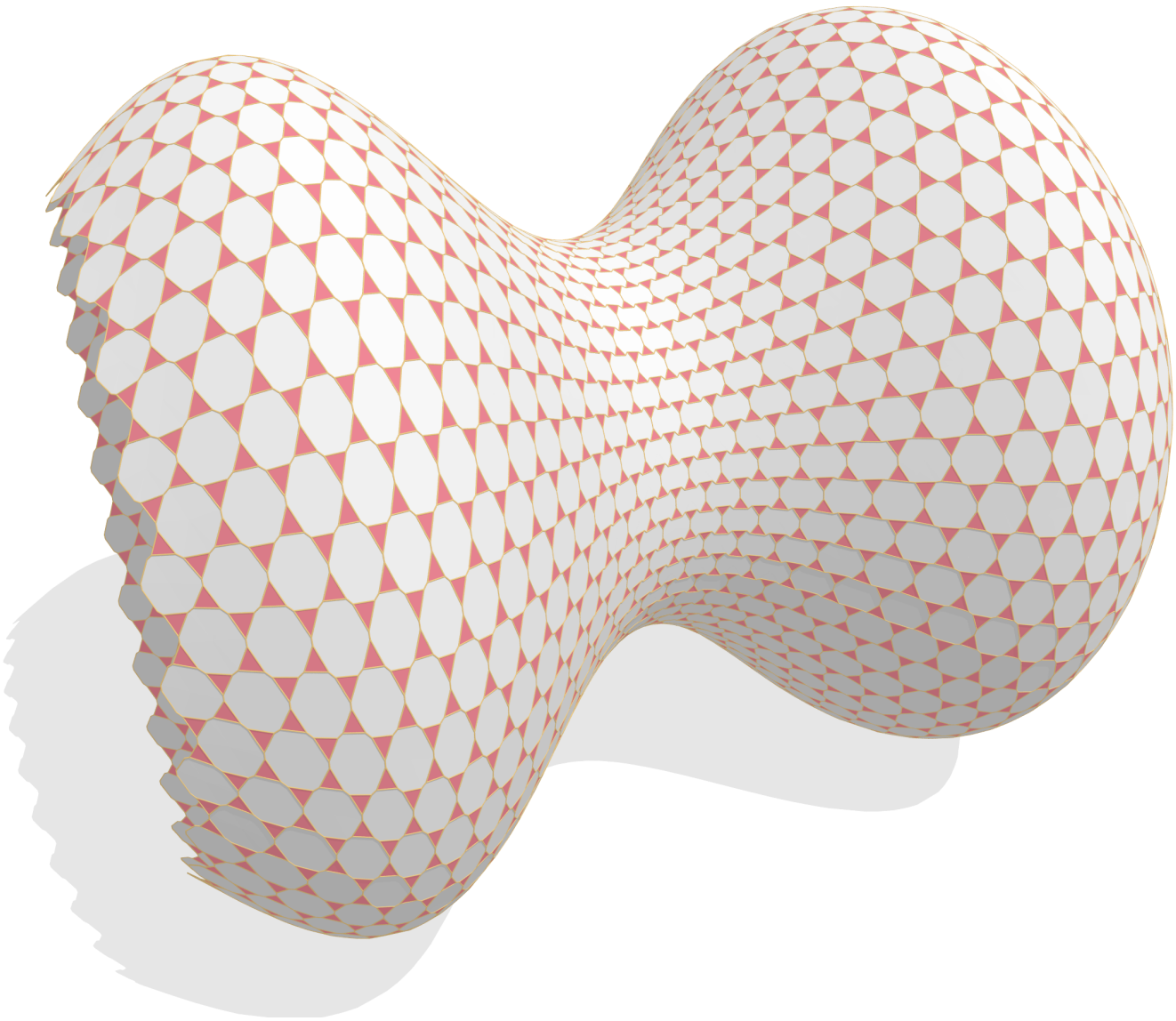

Figure 5: *A* $(3, 12, 12)$ *pattern using face and edge midpoint symmetries.*

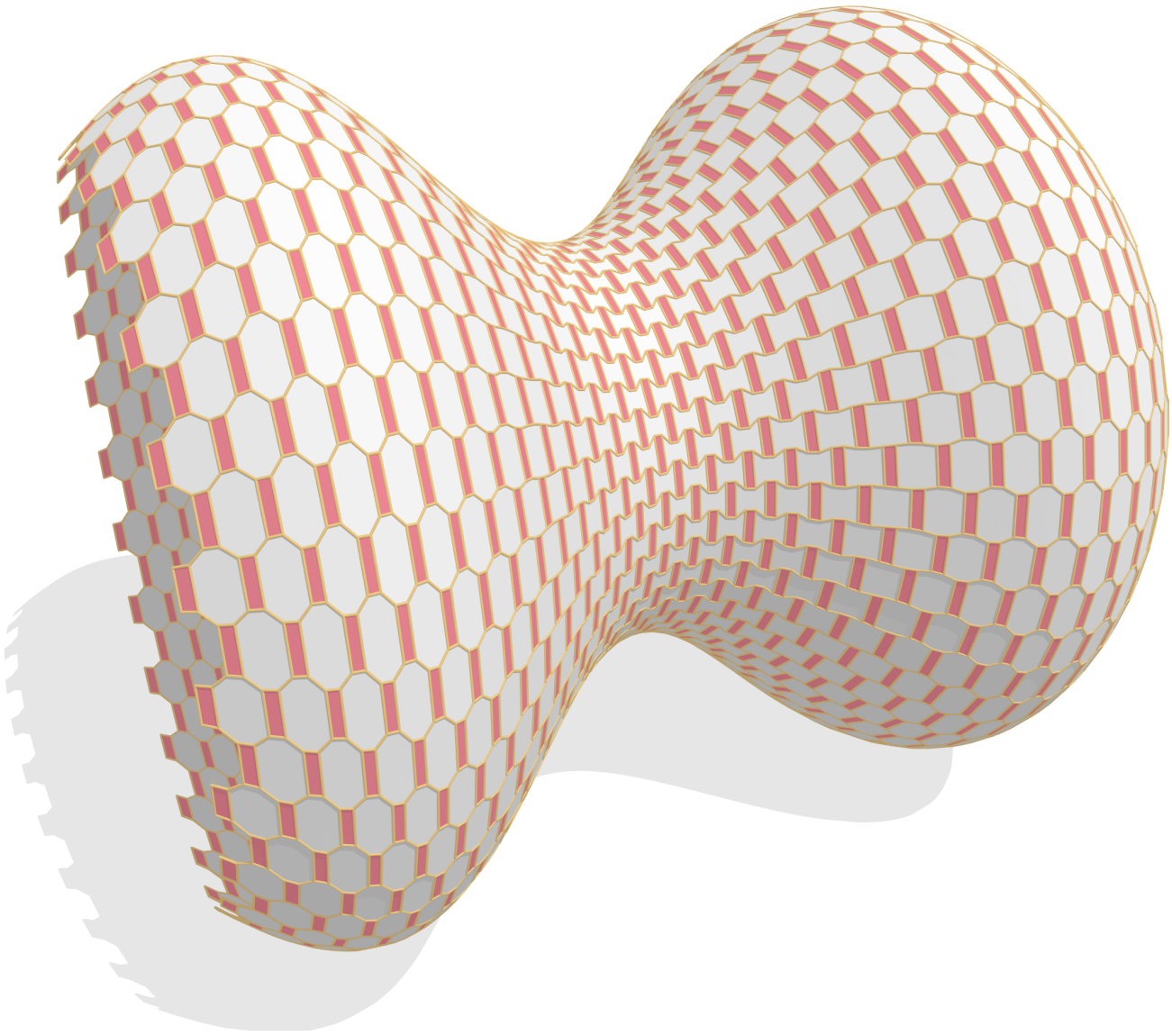

Figure 6: *A* $(4, 8, 8)$ *pattern using face symmetries.*

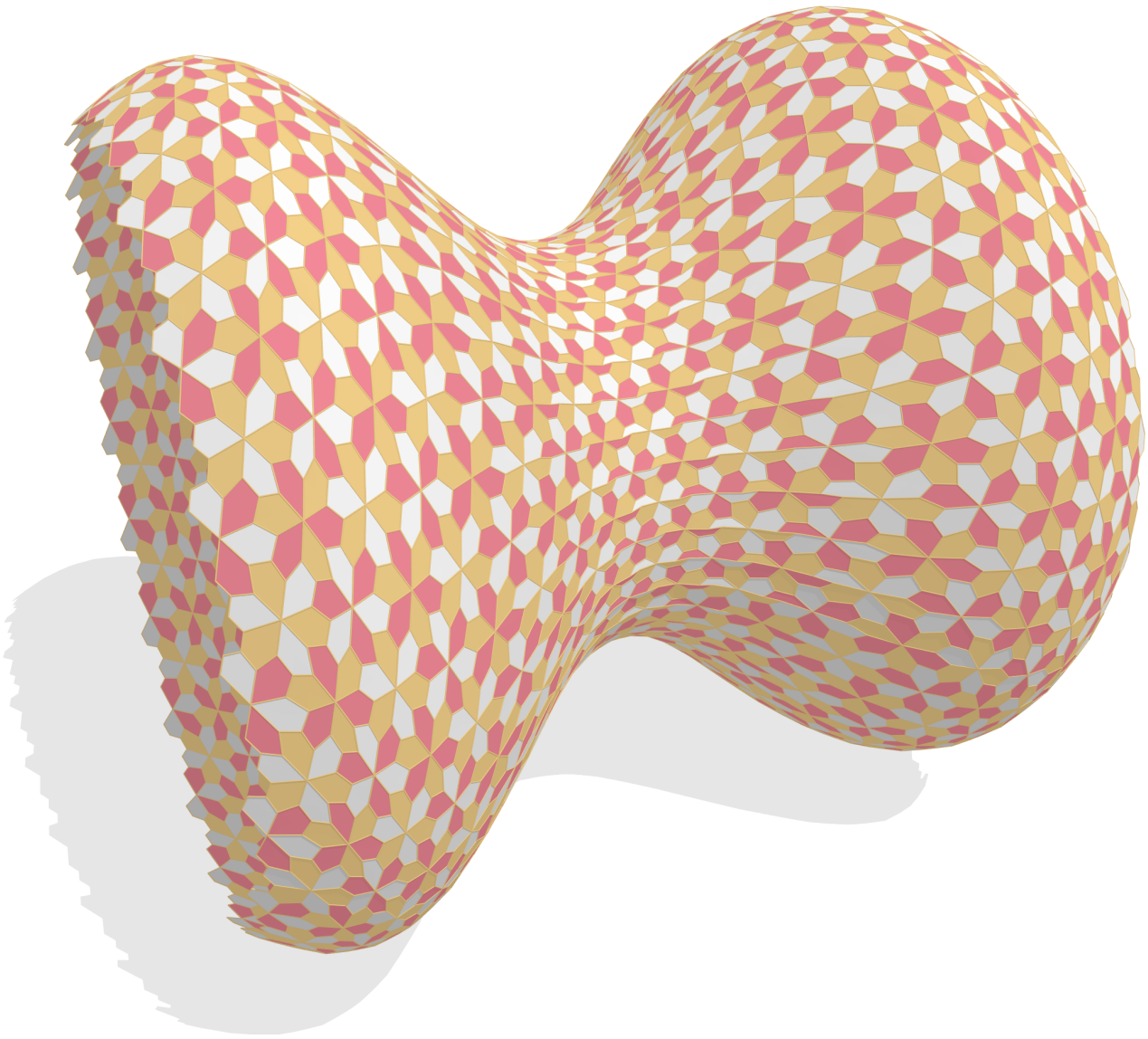

Figure 7: *A* $(3^4, 6)^*$ *pattern using vertex symmetries.*

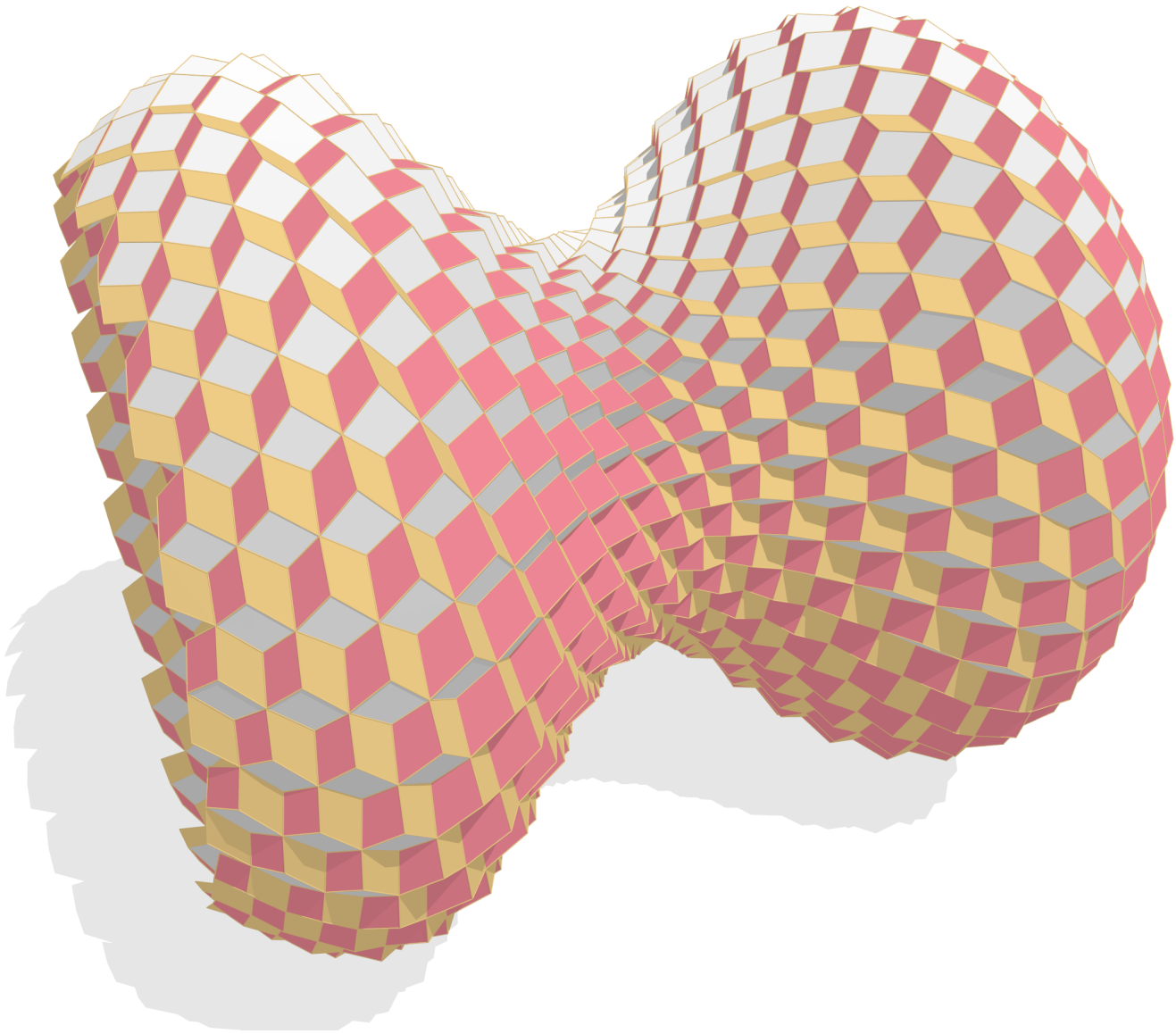

Figure 8: *A* $(3, 6, 3, 6)^*$ *pattern using symmetries with respect to an edge.*

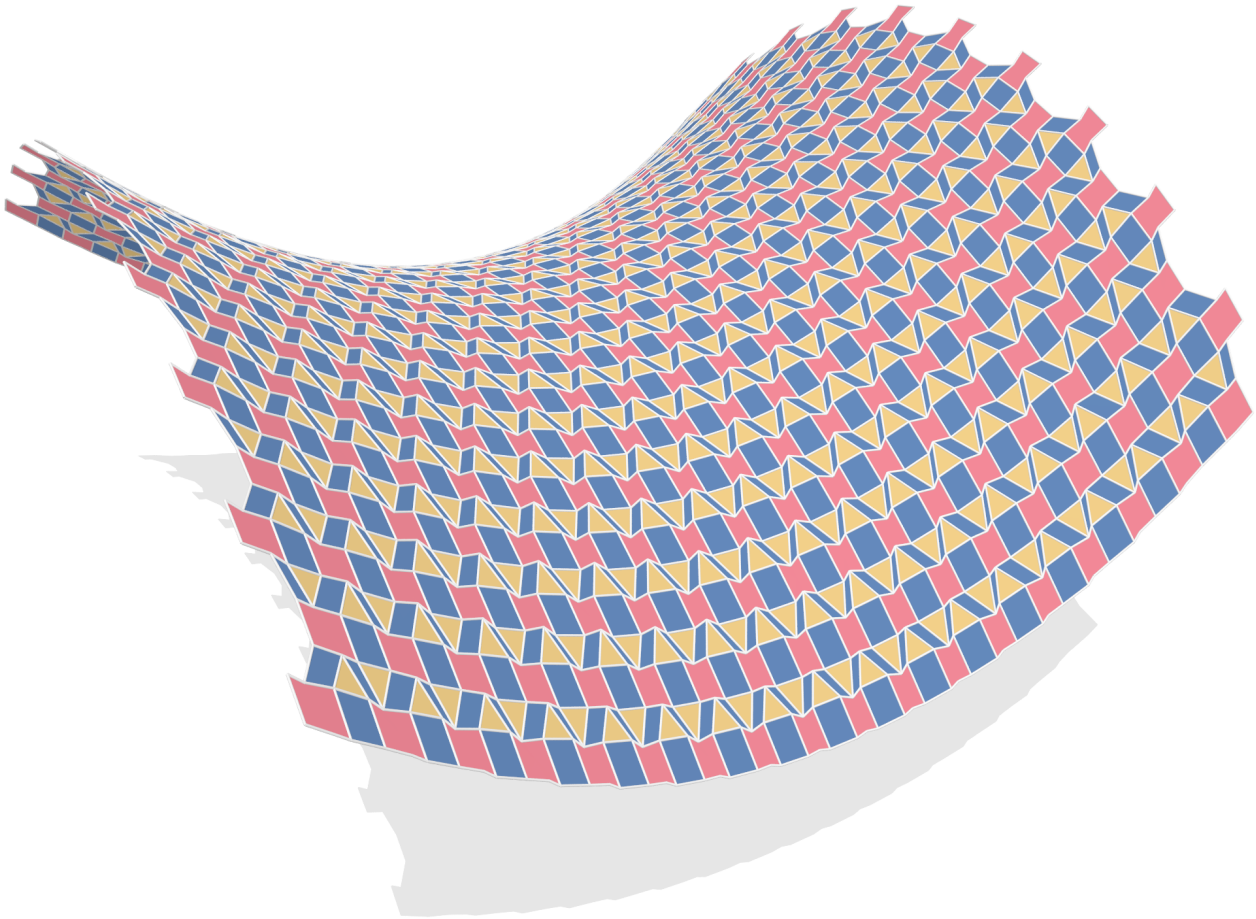

Figure 9: *A* $(3, 4, 6, 4)$ *pattern using face symmetries.*

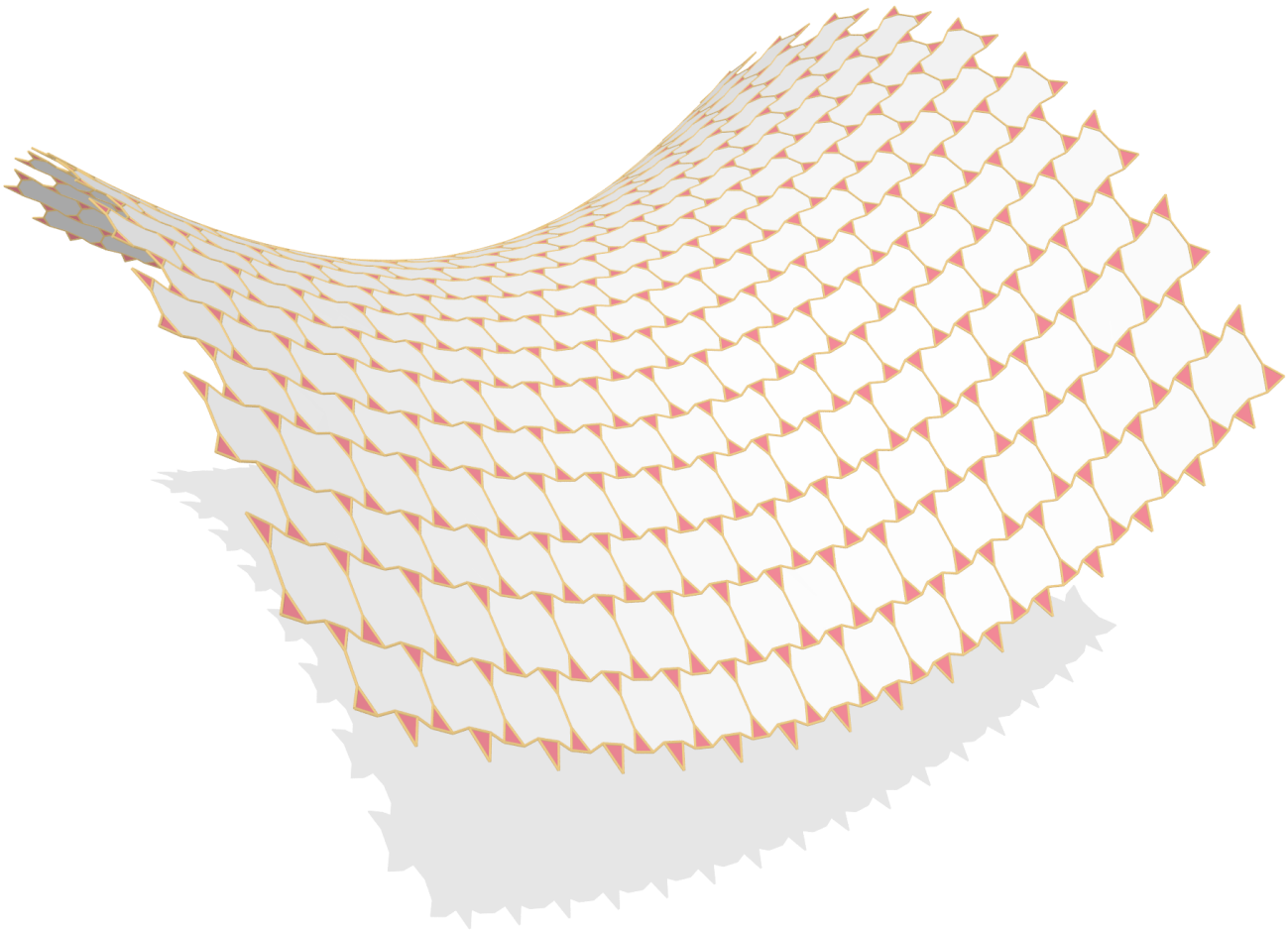

Figure 10: *A* $(3, 12, 12)$ *pattern using face and edge midpoint symmetries.*

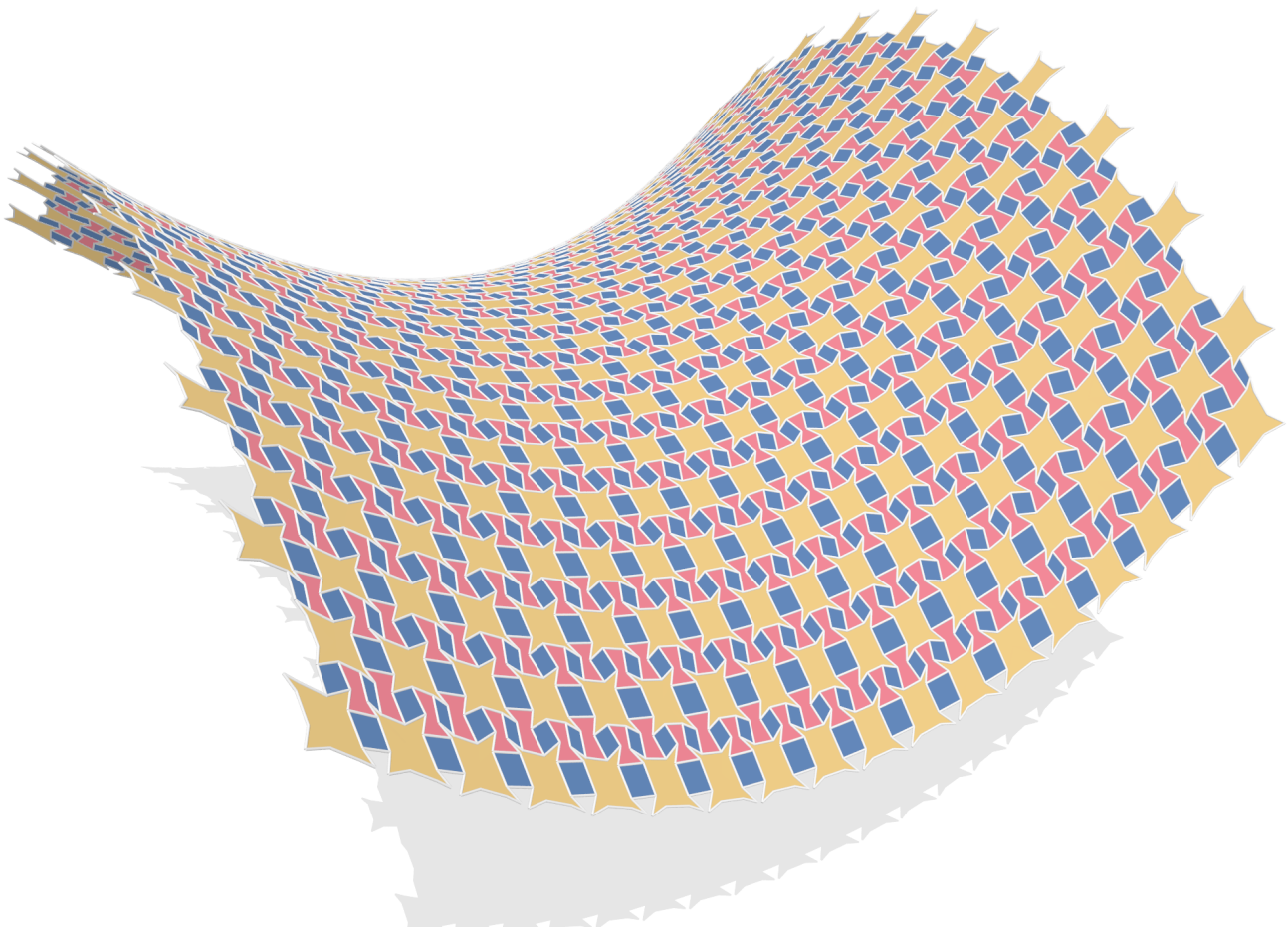

Figure 11: *A* $(4, 6, 12)$ *pattern using face symmetries.*

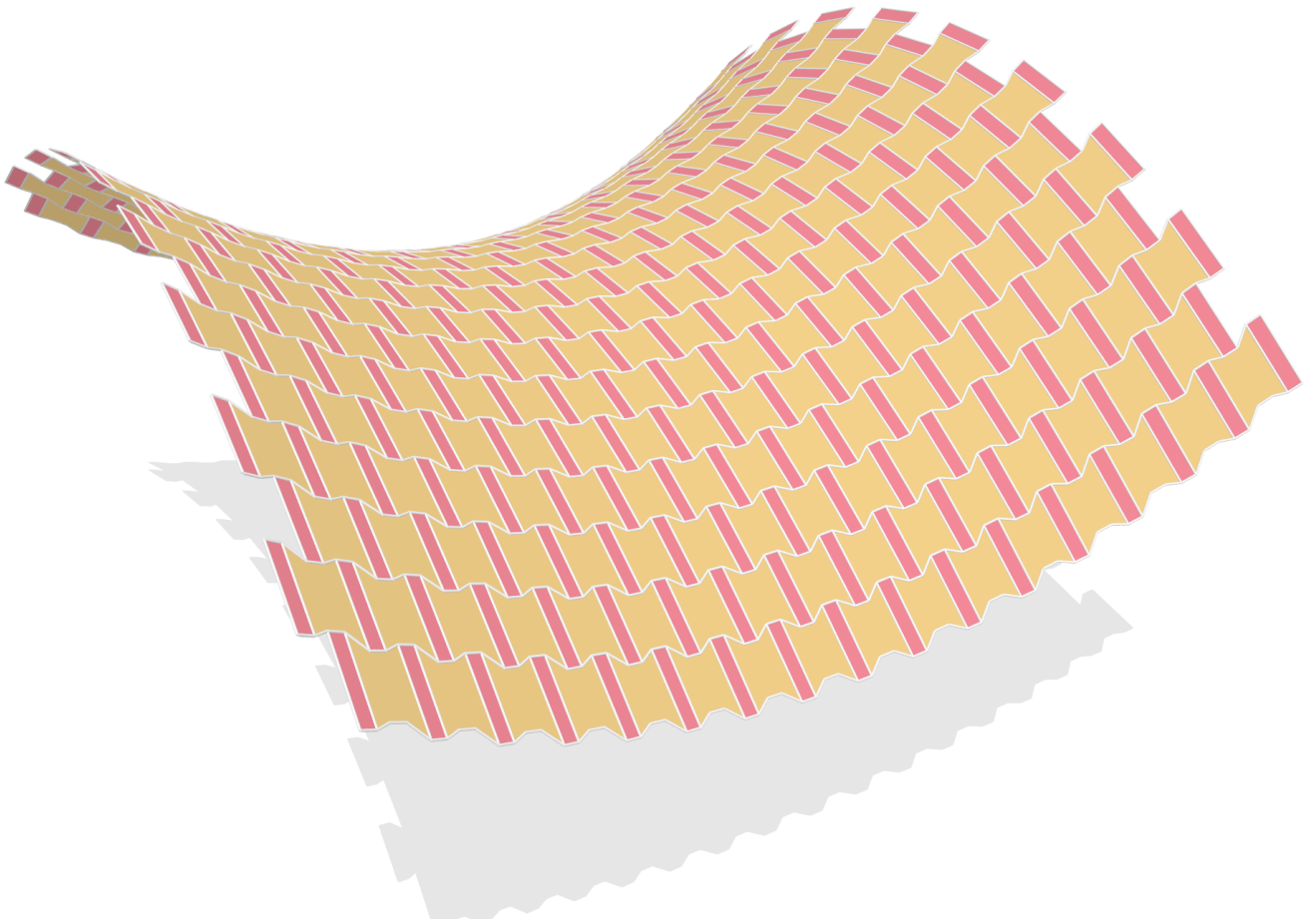

Figure 12: *A* $(4, 8, 8)$ *pattern using face symmetries.*

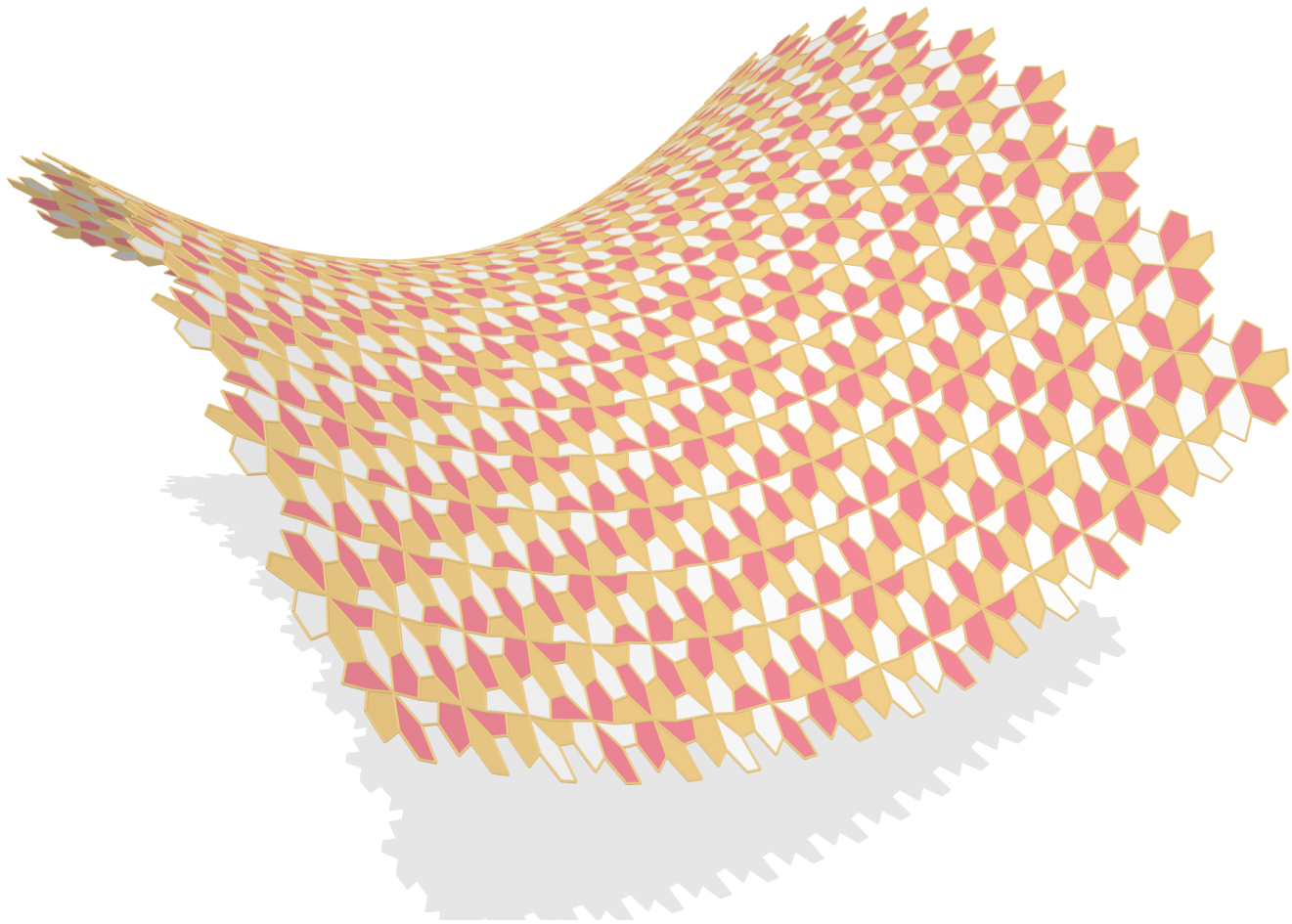

Figure 13: *A* $(3^4, 6)^*$ *pattern using vertex symmetries.*

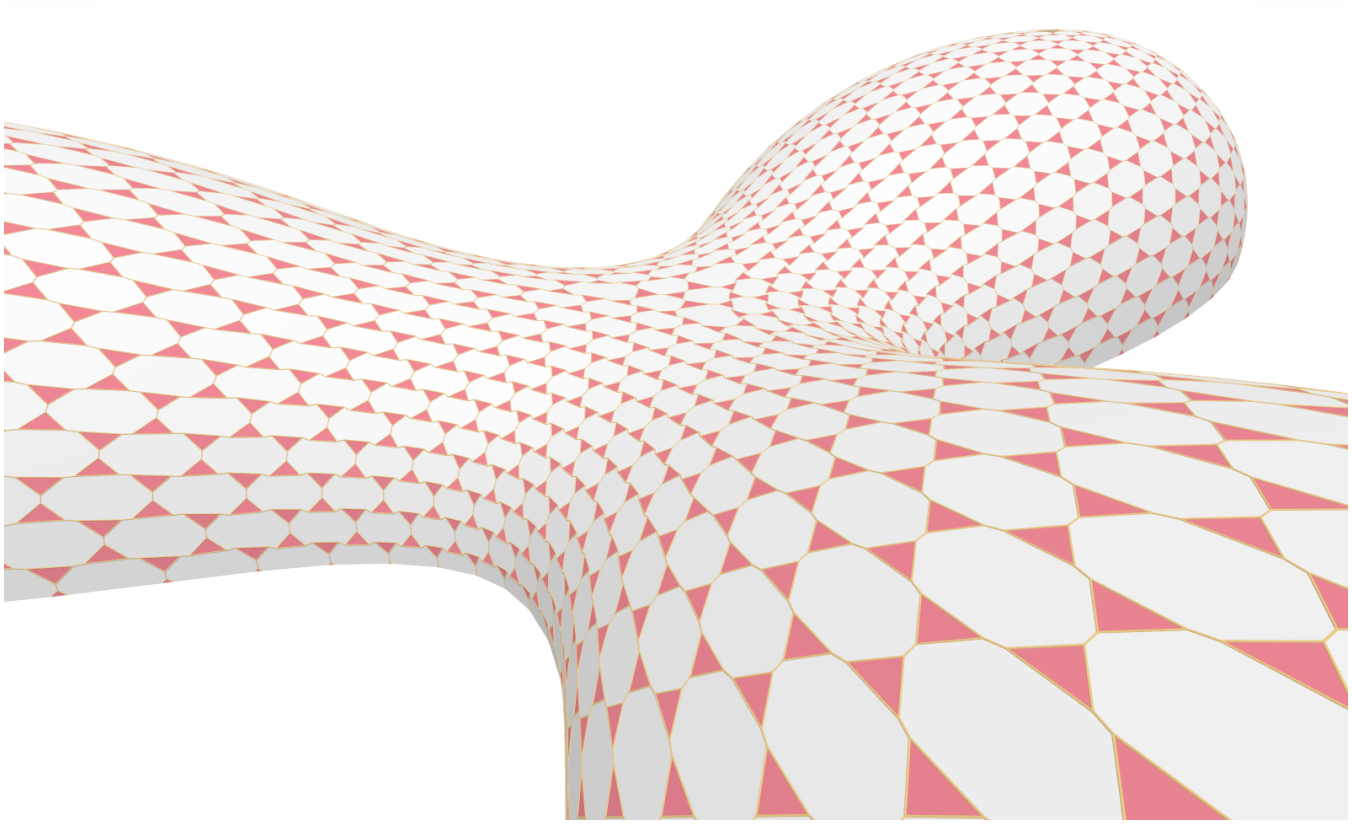

Figure 14: *A* $(3, 12, 12)$ *pattern using face and edge midpoint symmetries.*

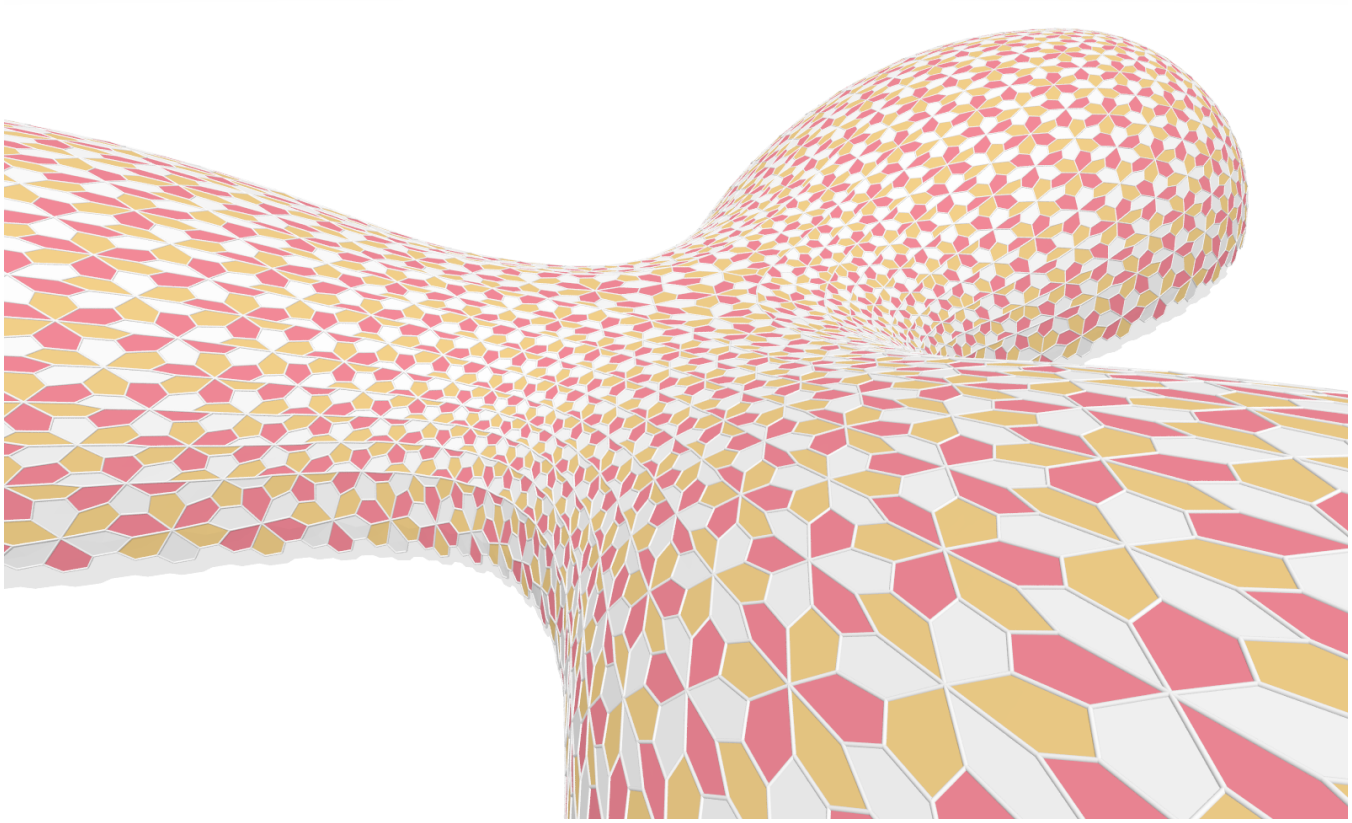

Figure 15: *A* $(3^4, 6)^*$ *pattern using vertex symmetries.*

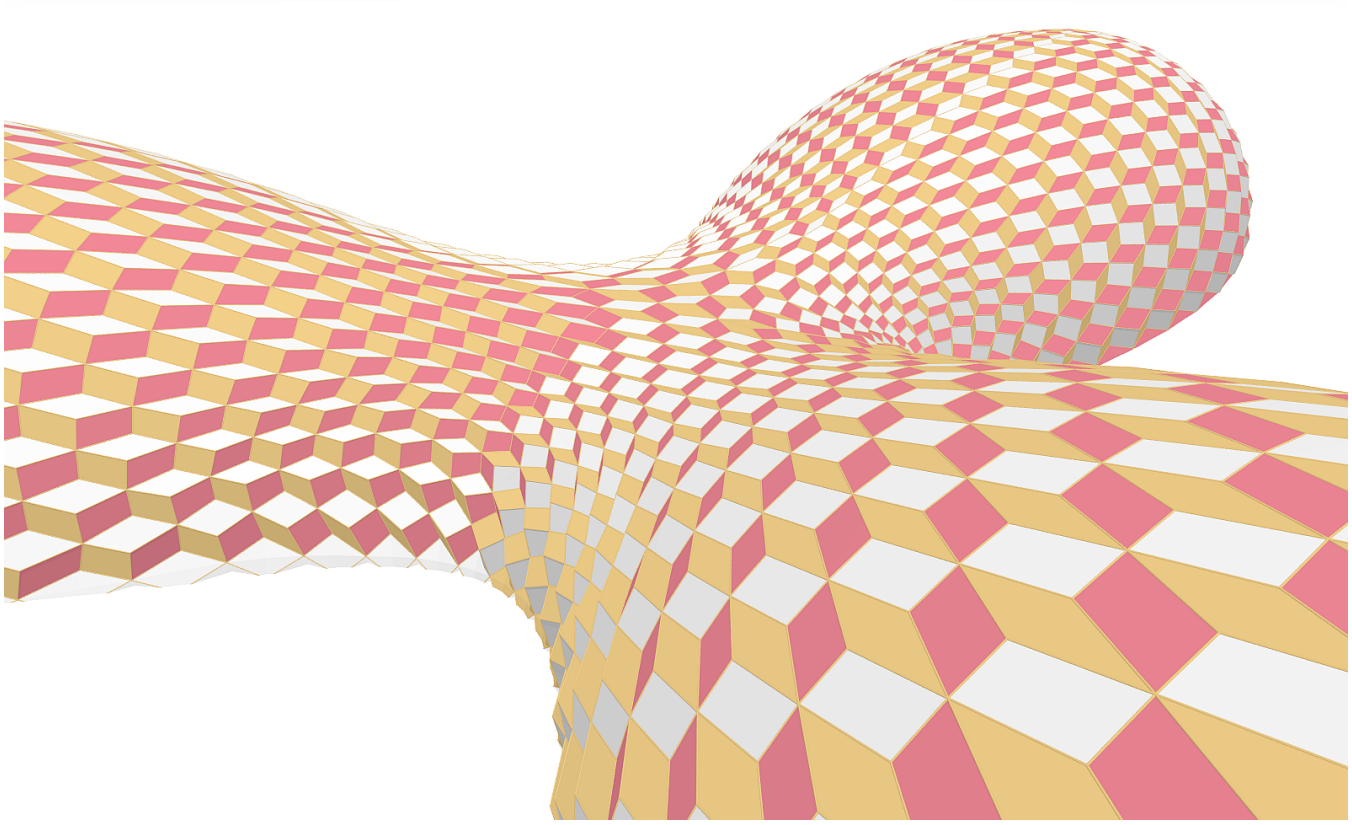

Figure 16: *A* $(3, 6, 3, 6)^*$ *pattern using symmetries with respect to an edge.*

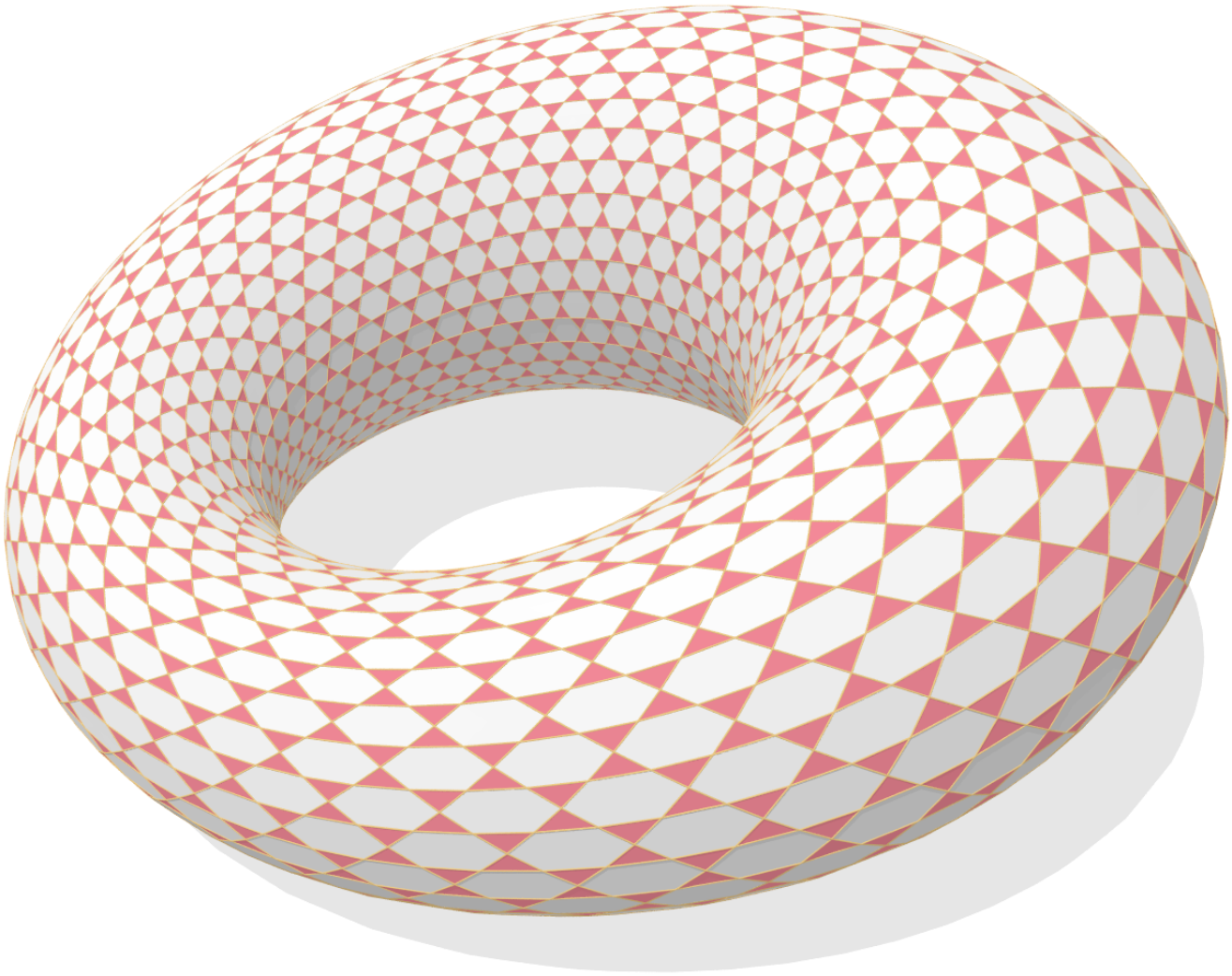

Figure 17: *A* $(3, 6, 3, 6)$ *pattern using vertex symmetries.*

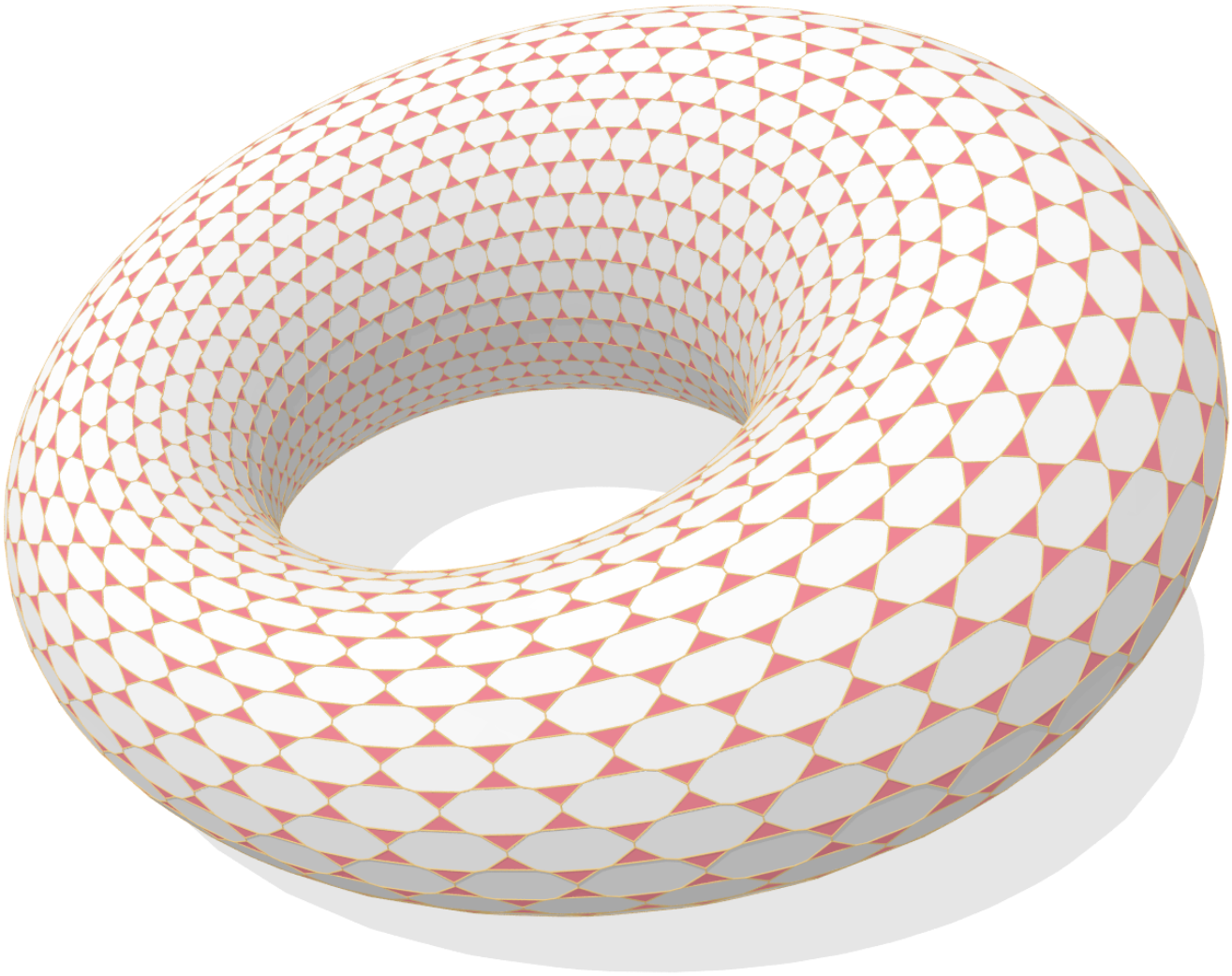

Figure 18: *A* $(3, 12, 12)$ *pattern using face and edge midpoint symmetries.*

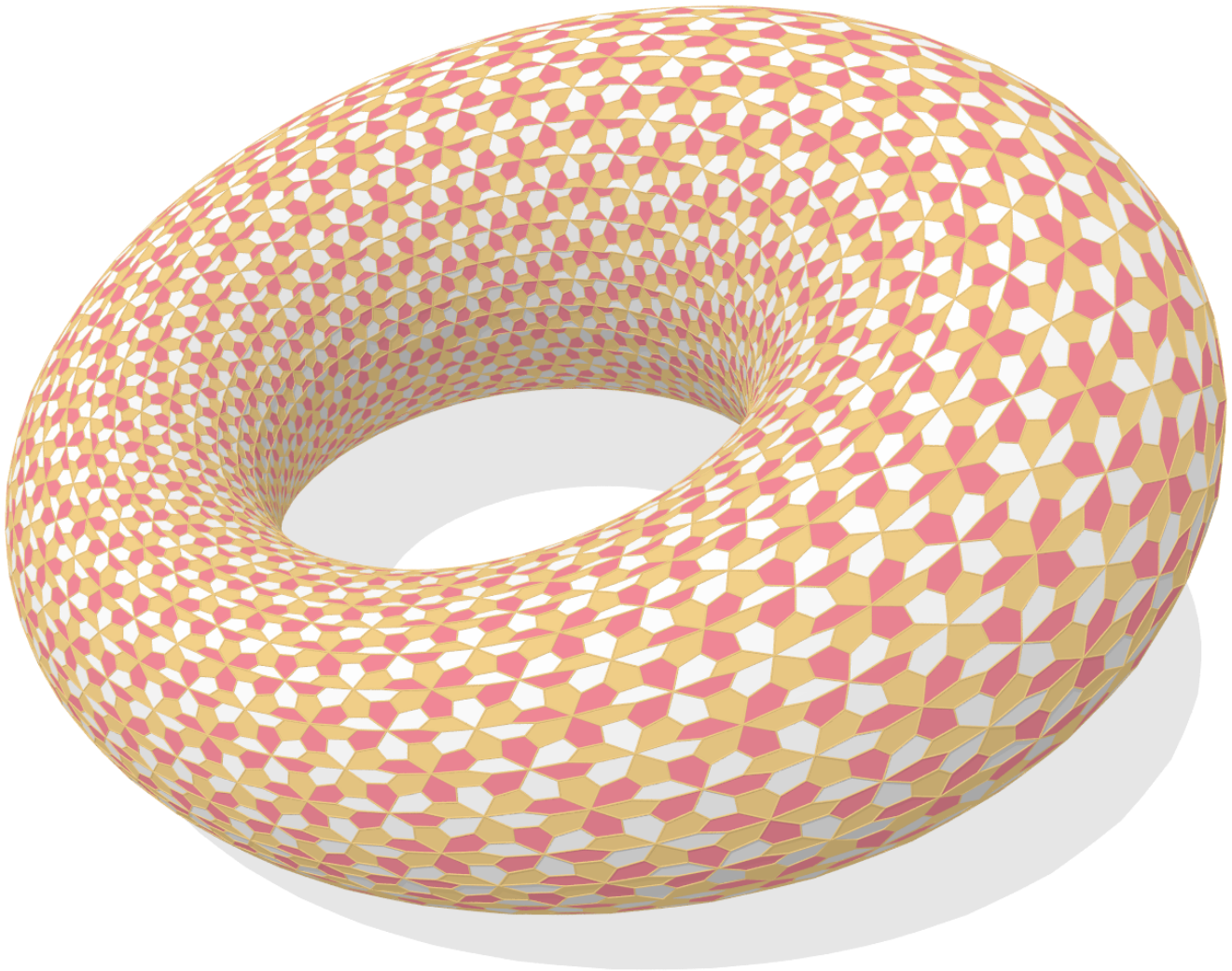

Figure 19: *A* $(3^4, 6)^*$ *pattern using vertex symmetries.*

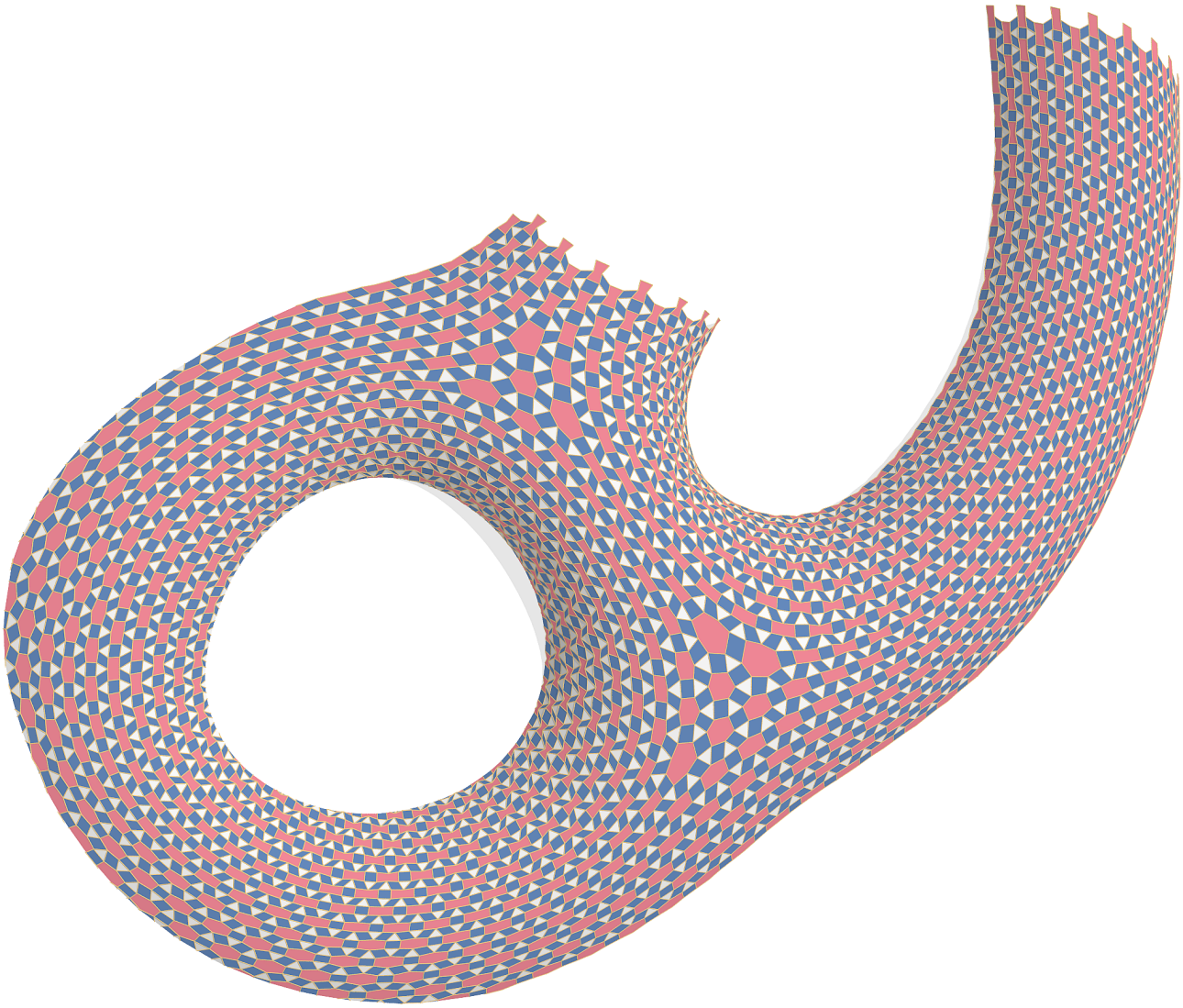

Figure 20: *A* $(3, 4, 6, 4)$ *pattern using face symmetries.*

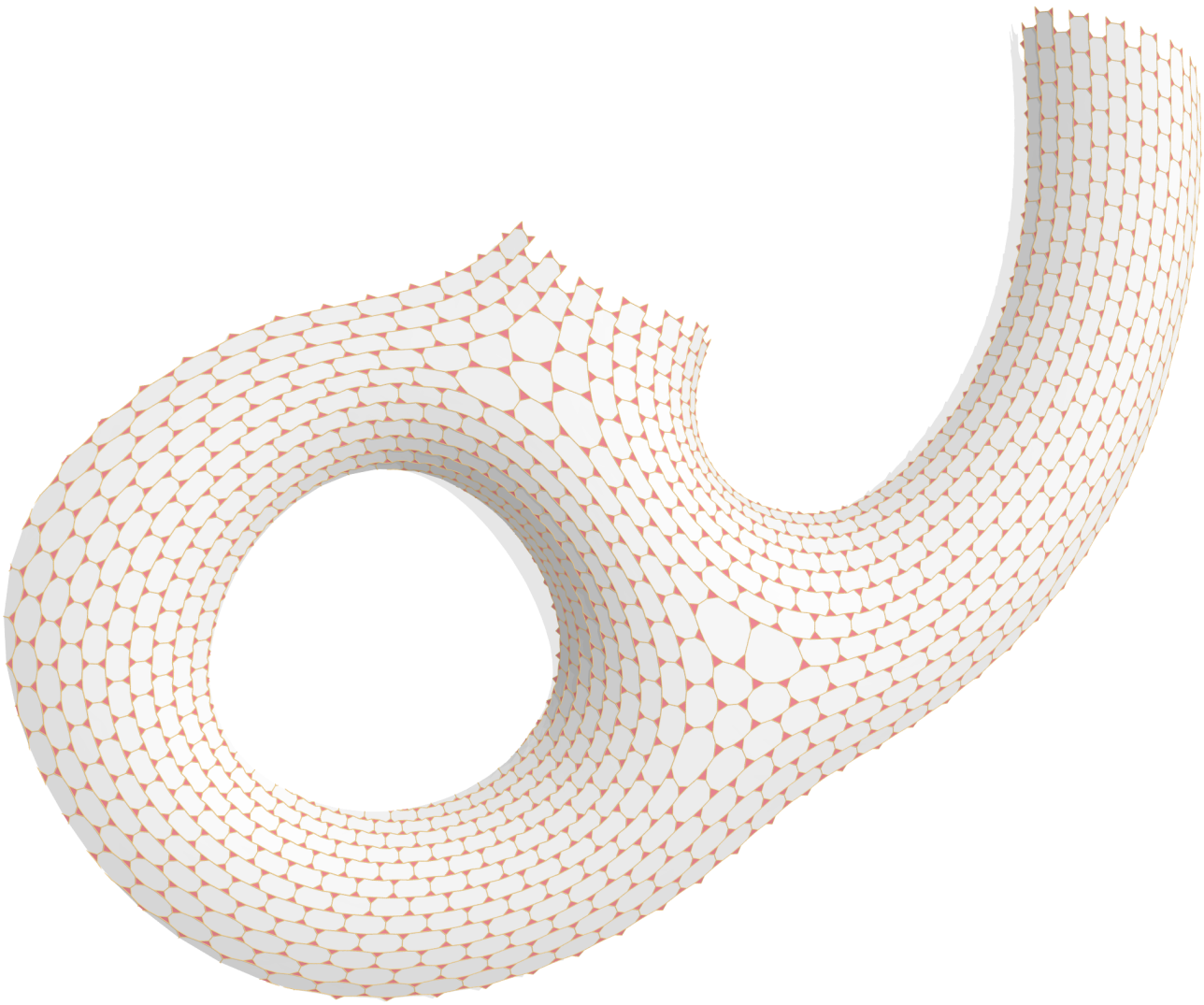

Figure 21: *A* $(3, 12, 12)$ *pattern using face and edge midpoint symmetries.*

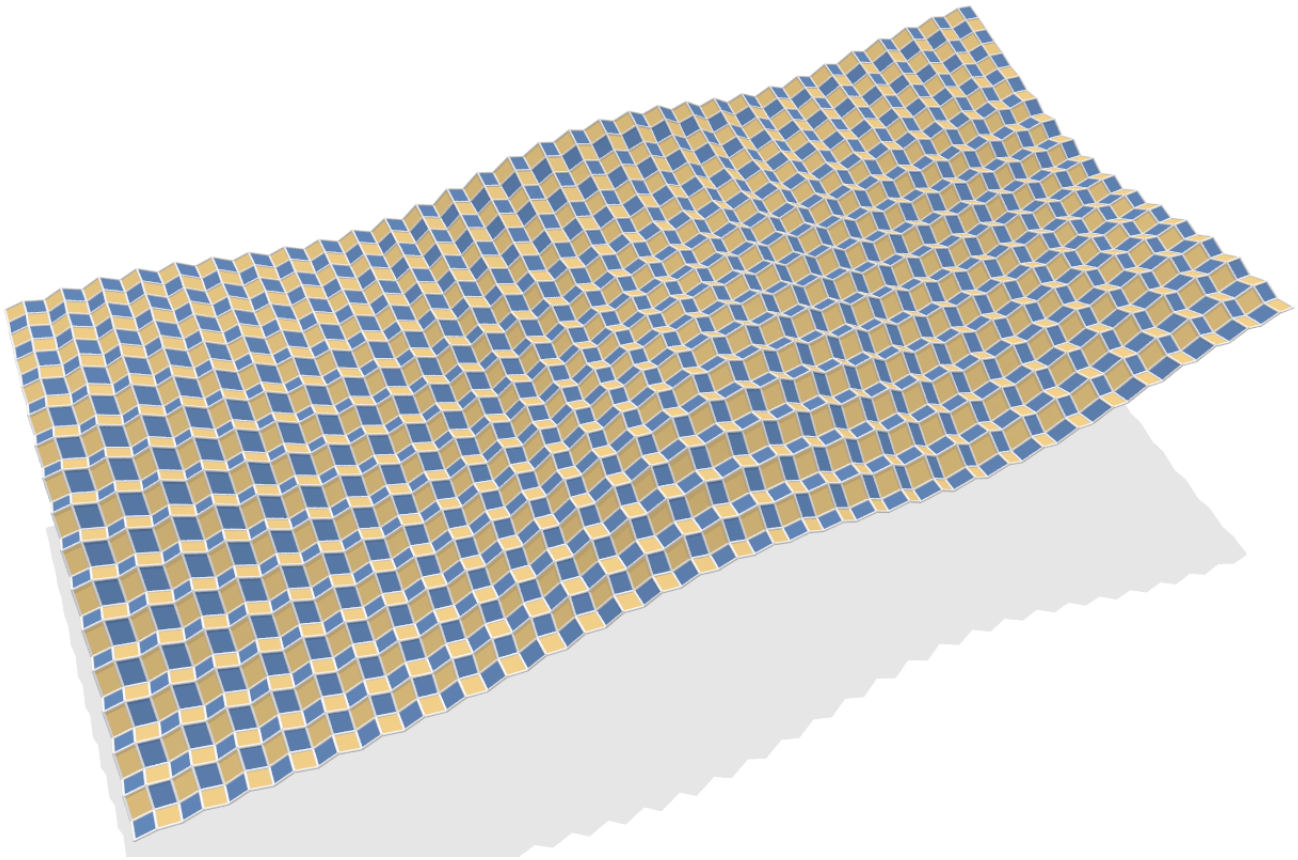

Figure 22: *A quad pattern using face symmetries.*

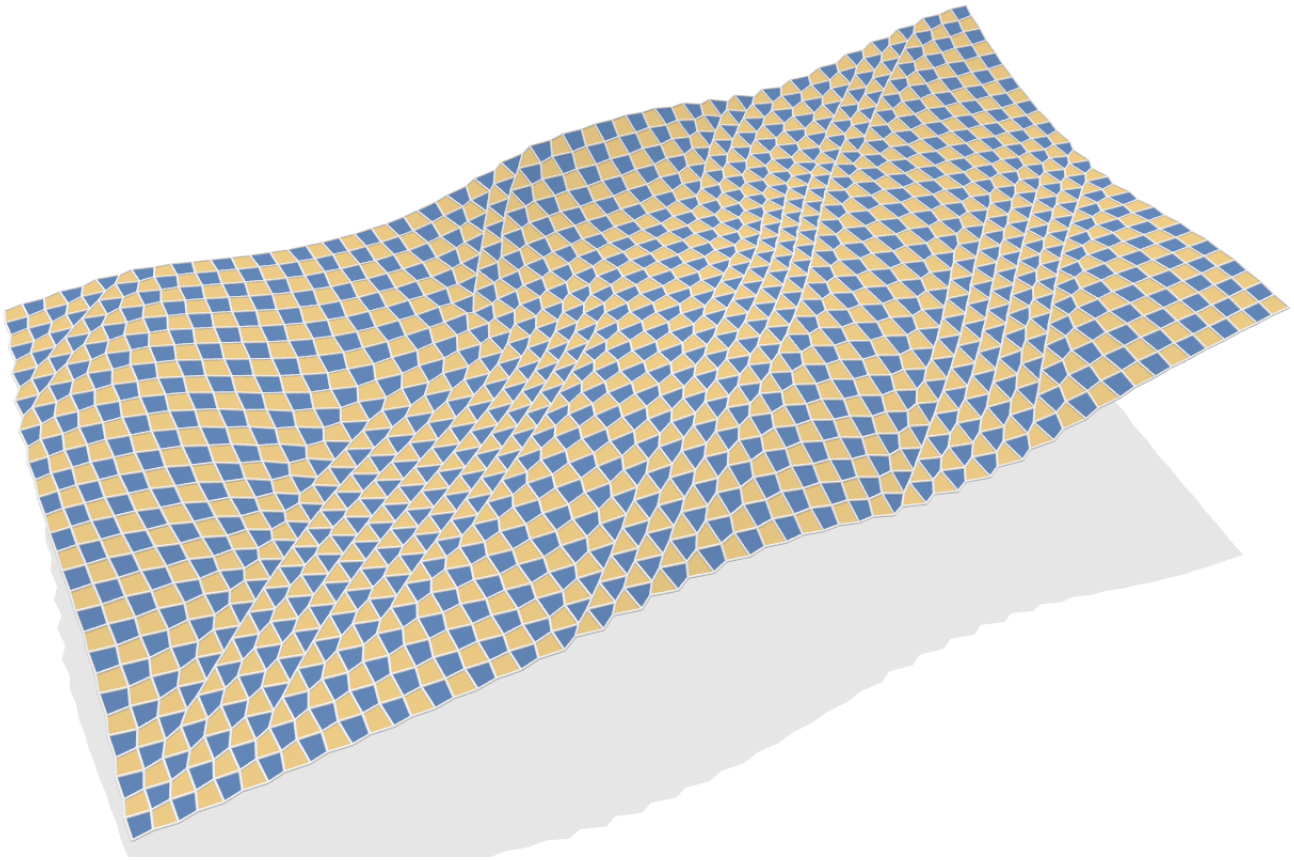

Figure 23: *A quad pattern using edge midpoint symmetries.*

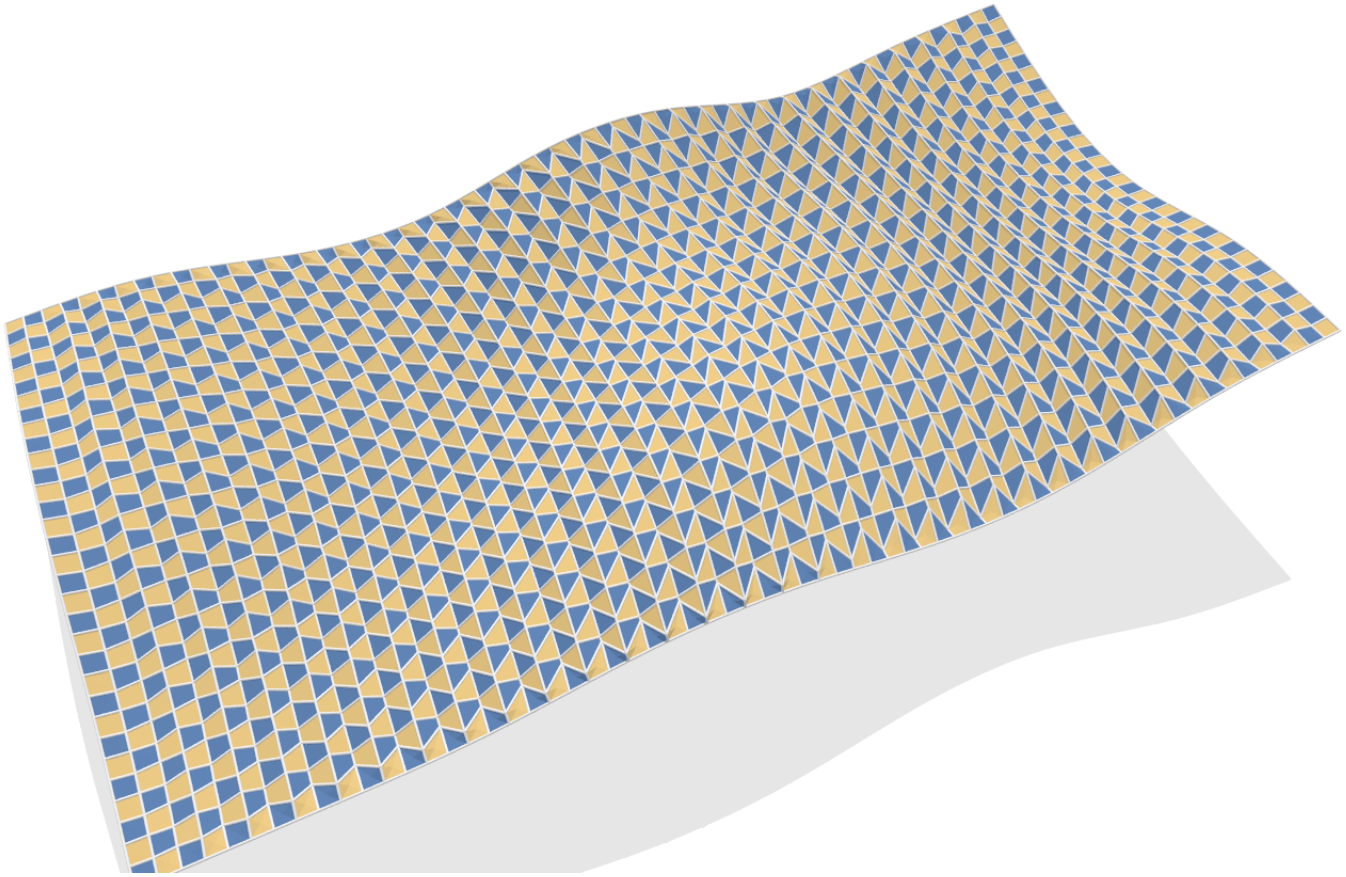

Figure 24: *A quad pattern using edge midpoint symmetries on one family of edges and symmetries with respect an edge on the other family of edges.*

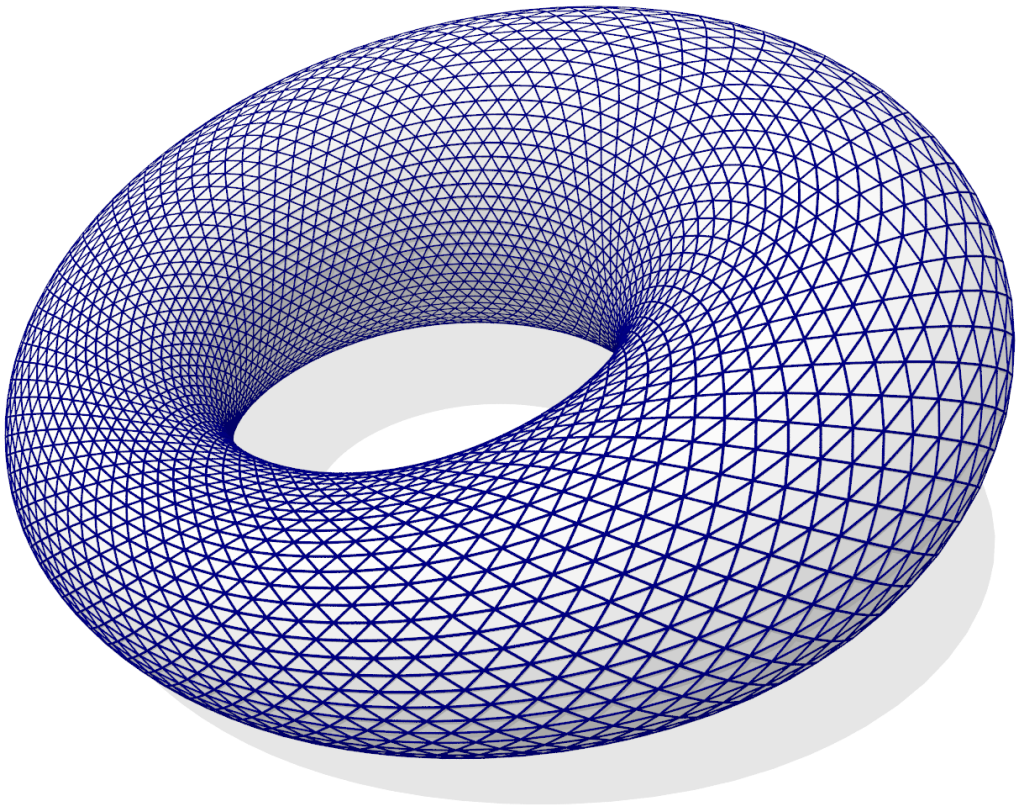

Figure 25: *The following figures show a workflow of creating a polyhedral pattern based on the reference triangle mesh shown here.*

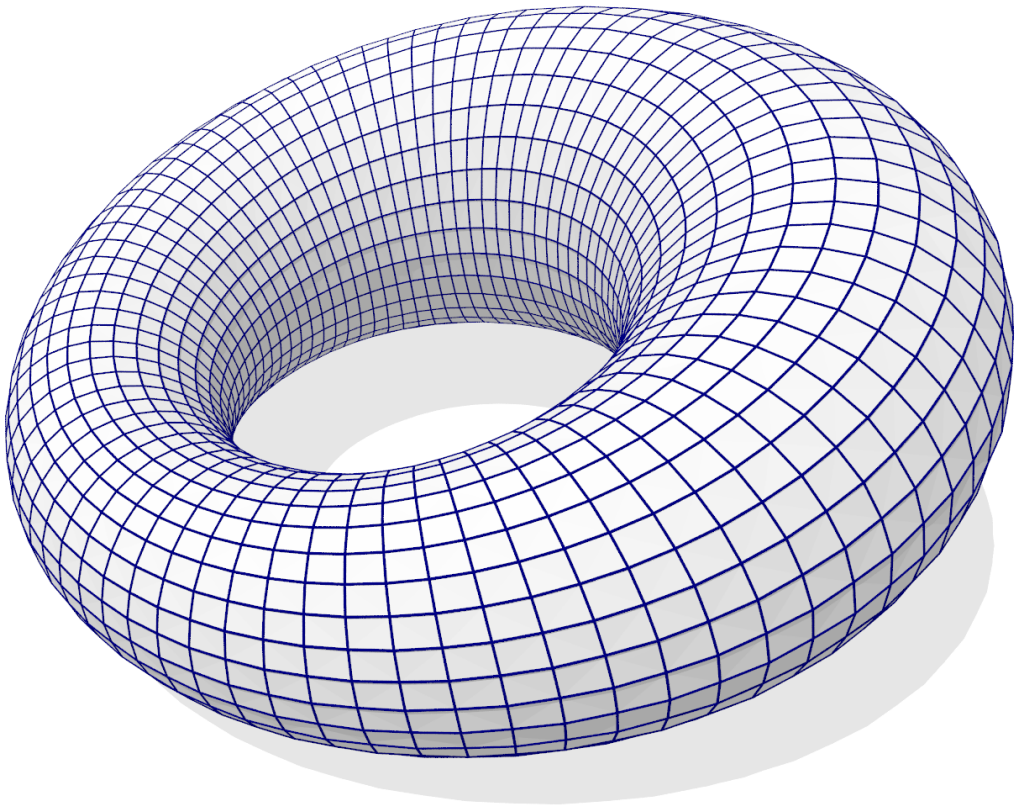

Figure 26: *A quad mesh is created based on the reference mesh shown in Figure 25.*

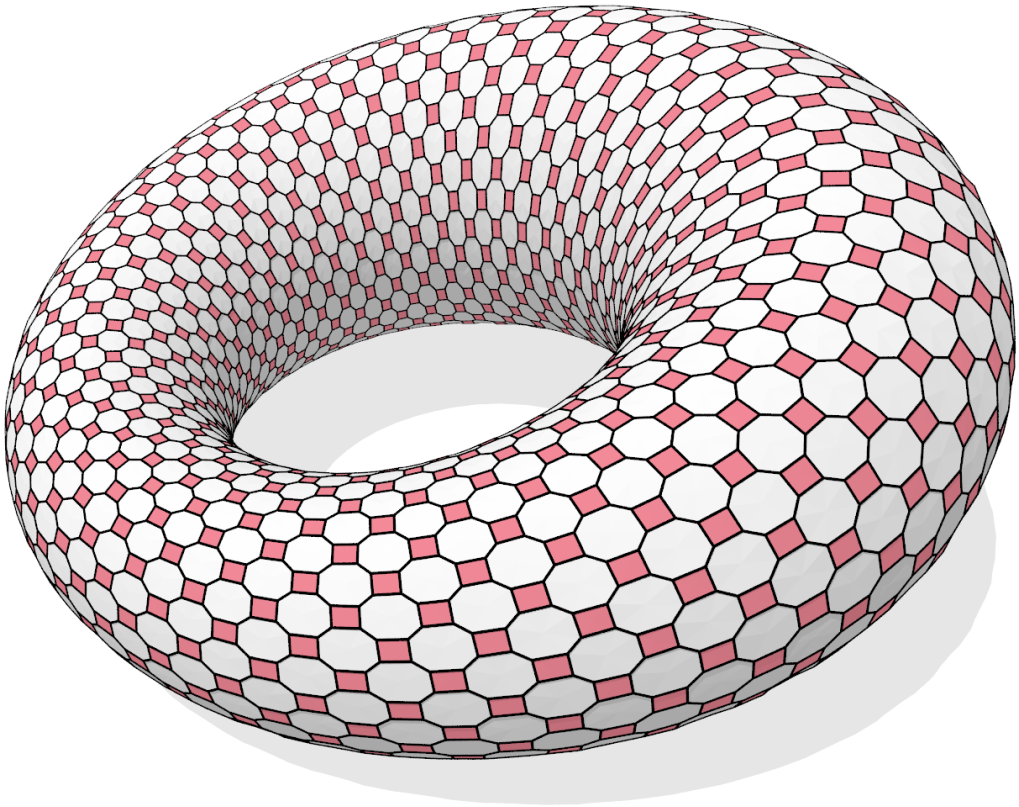

Figure 27: *An initial* $(4, 8, 8)$ *pattern mesh is generated based on the quad mesh shown in Figure 26.*

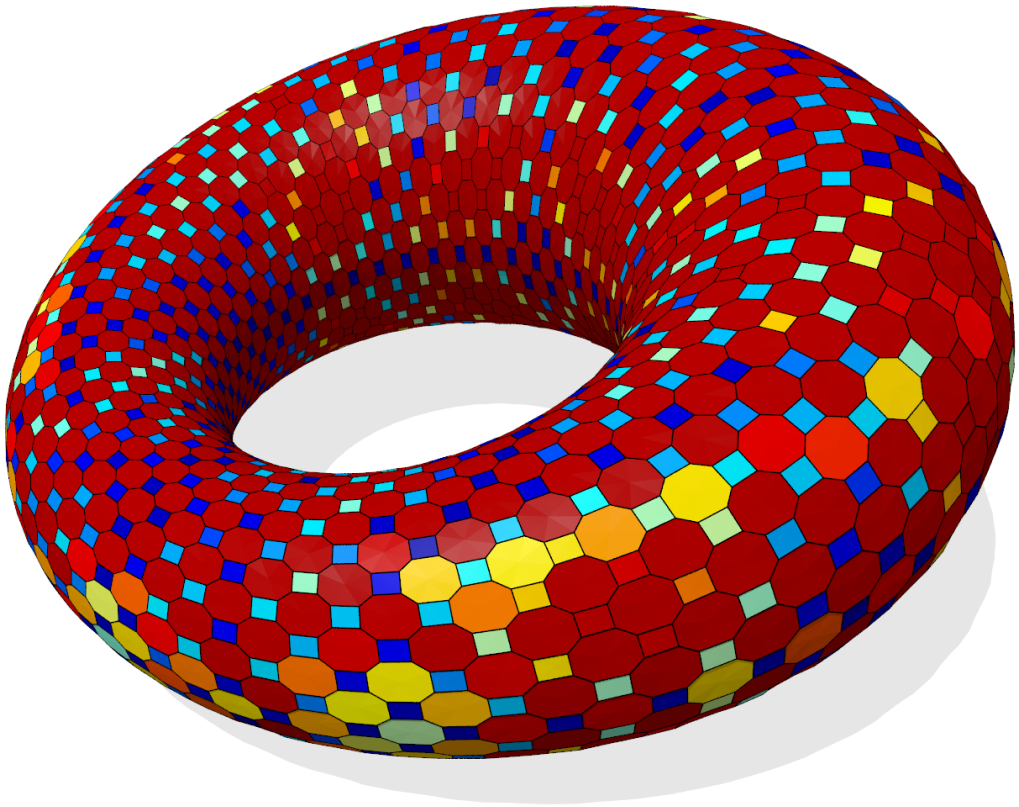

Figure 28: *The initial* $(4, 8, 8)$ *pattern shown in Figure 27 is not planar.*

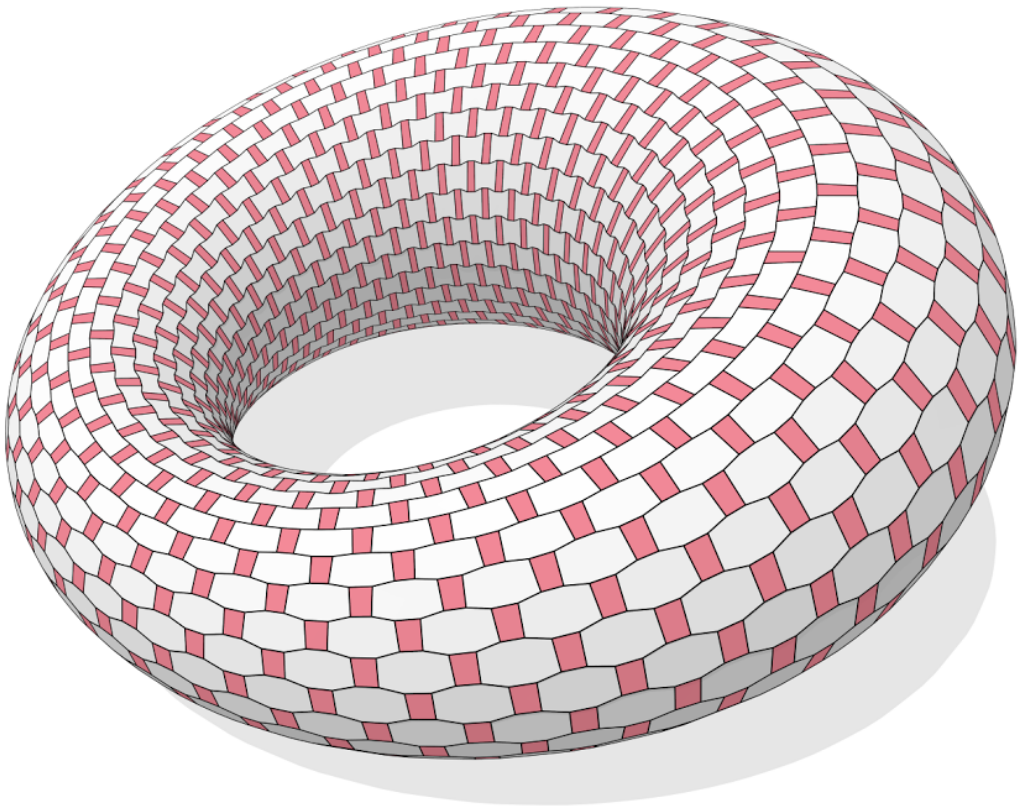

Figure 29: *The optimized* $(4, 8, 8$ *pattern from on the initial pattern shown in Figure 27.*

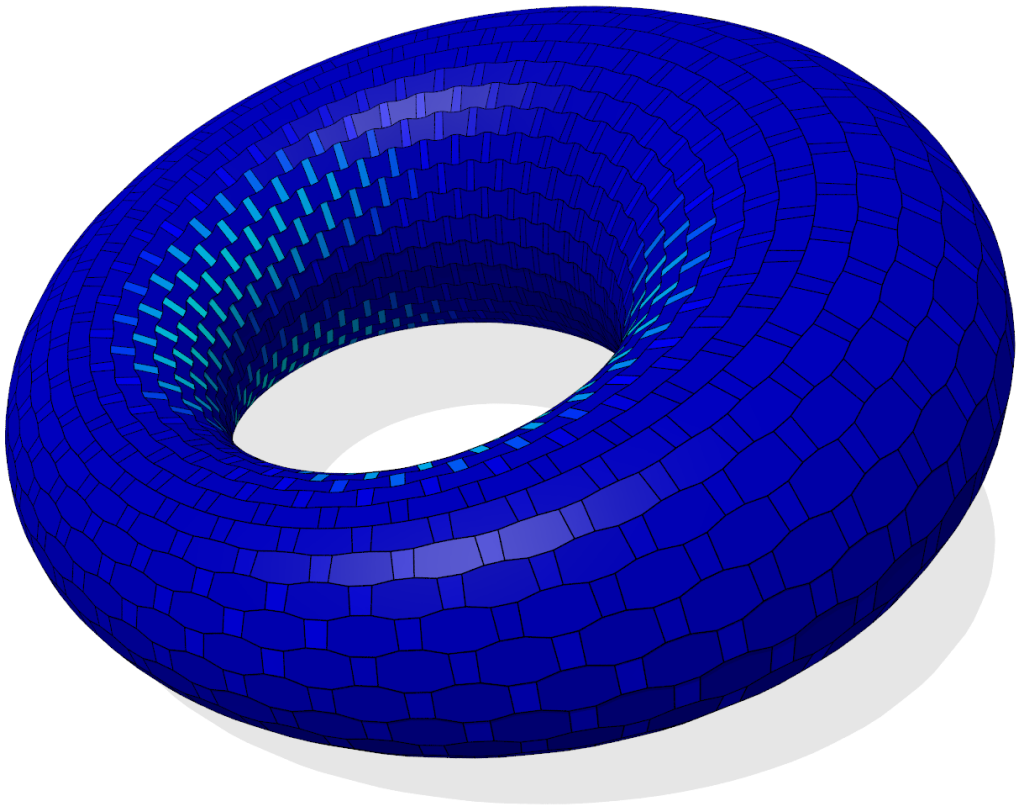

Figure 30: *The optimized pattern shown in Figure 29 is successfully planarized.*

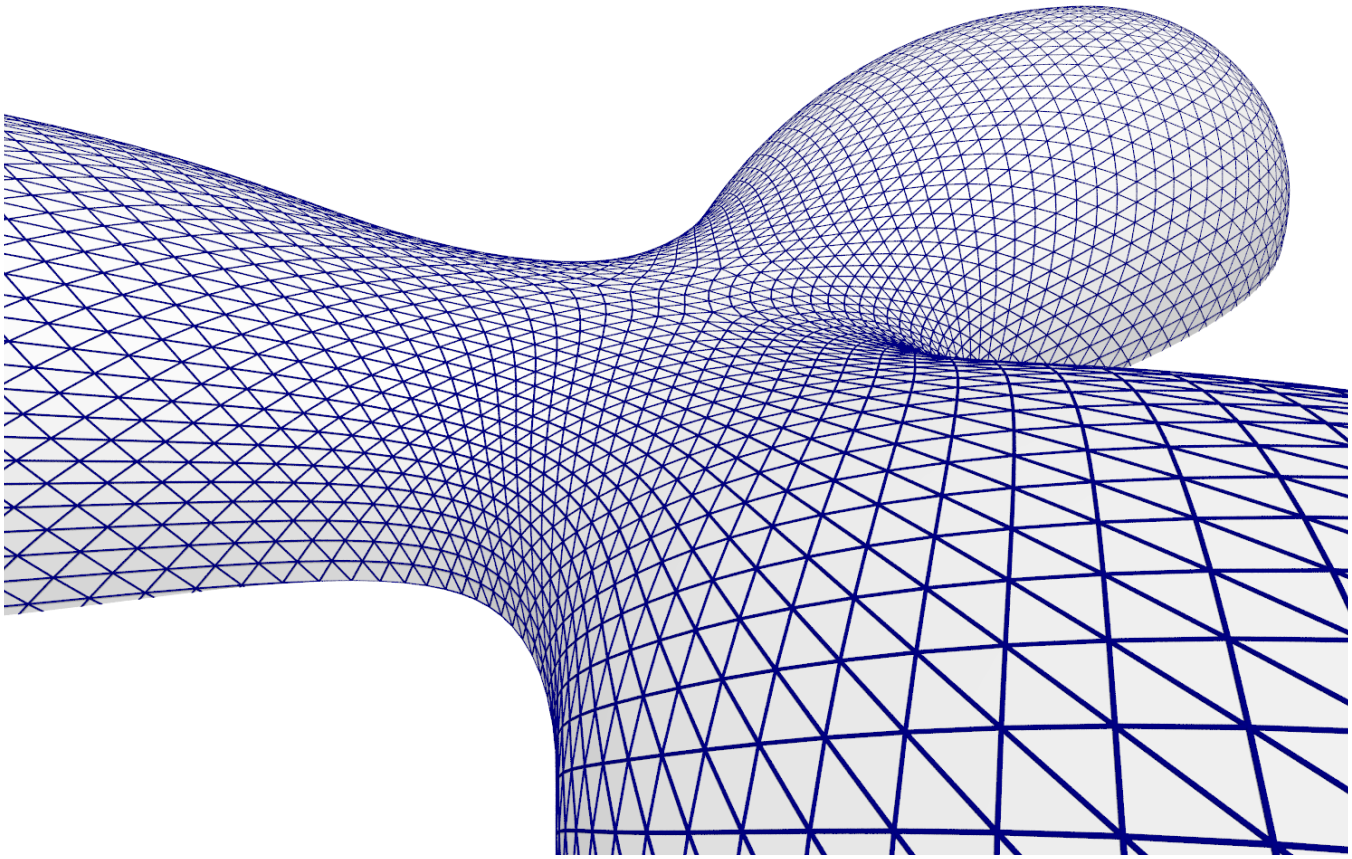

Figure 31: *The following figures show the workflow of creating a* $(3, 4, 6, 4)$ *pattern based on this triangle reference mesh.*

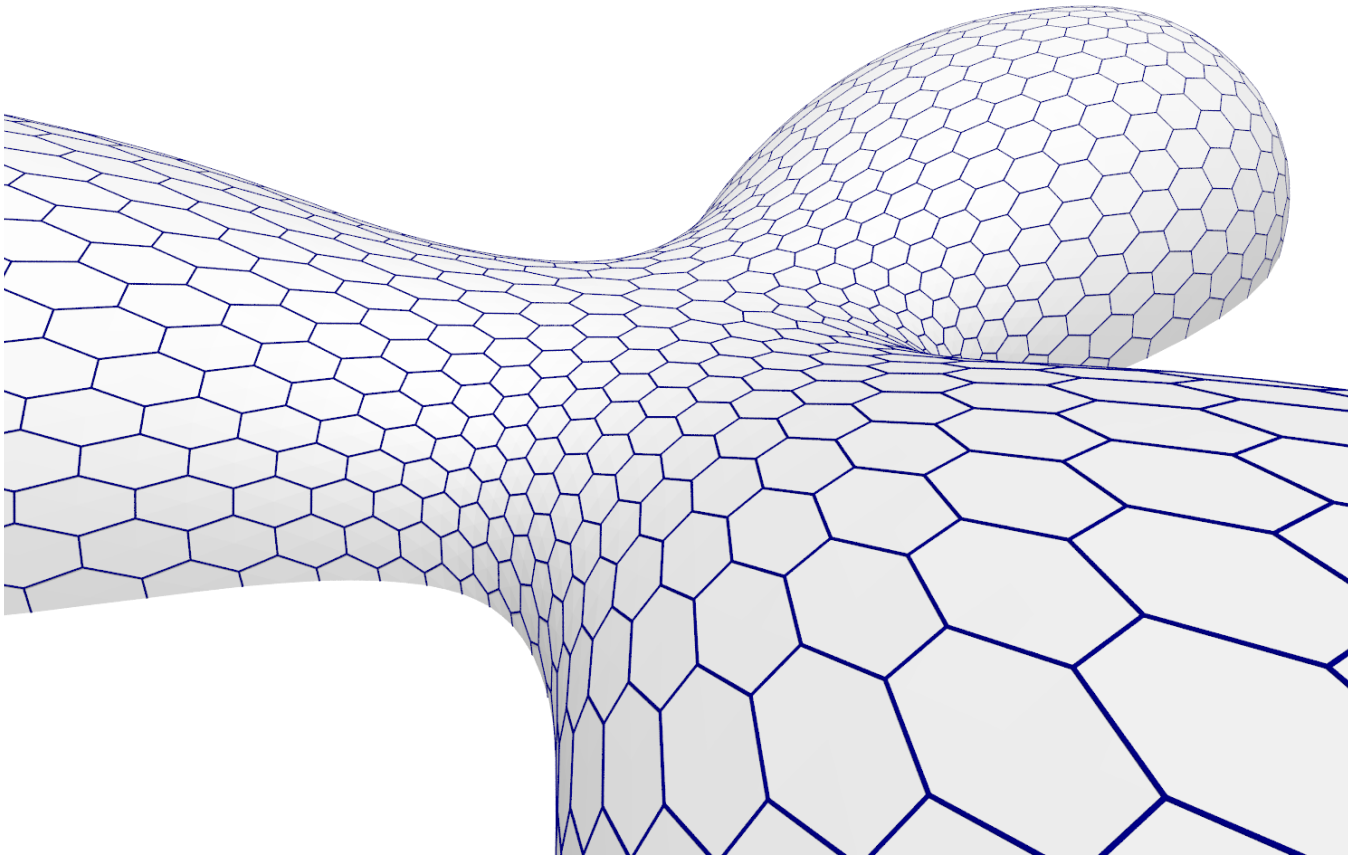

Figure 32: *A hex mesh is generated based on the reference mesh shown in Figure 31.*

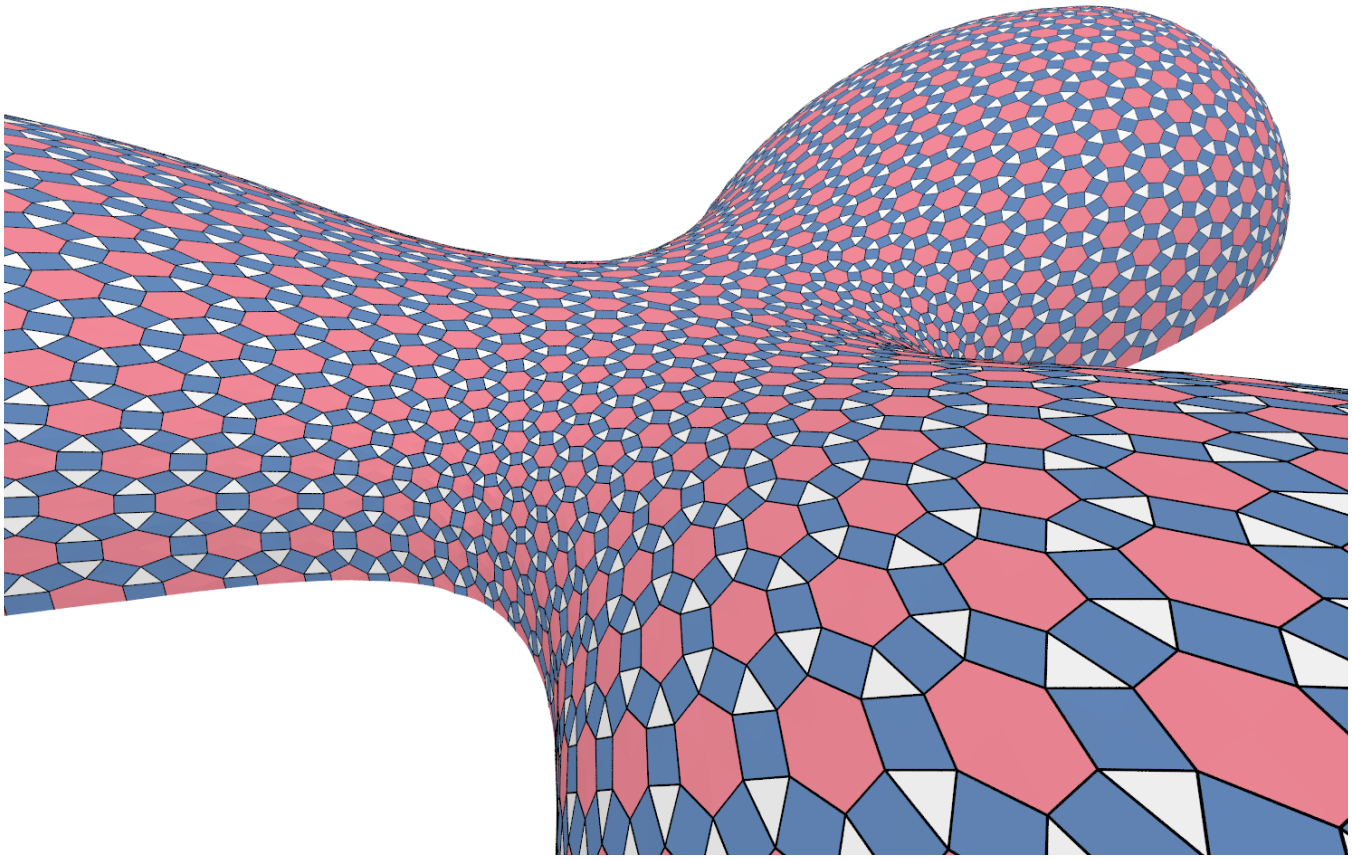

Figure 33: *An initial* $(3, 4, 6, 4)$ *pattern mesh is created based on the hex mesh shown in Figure 32.*

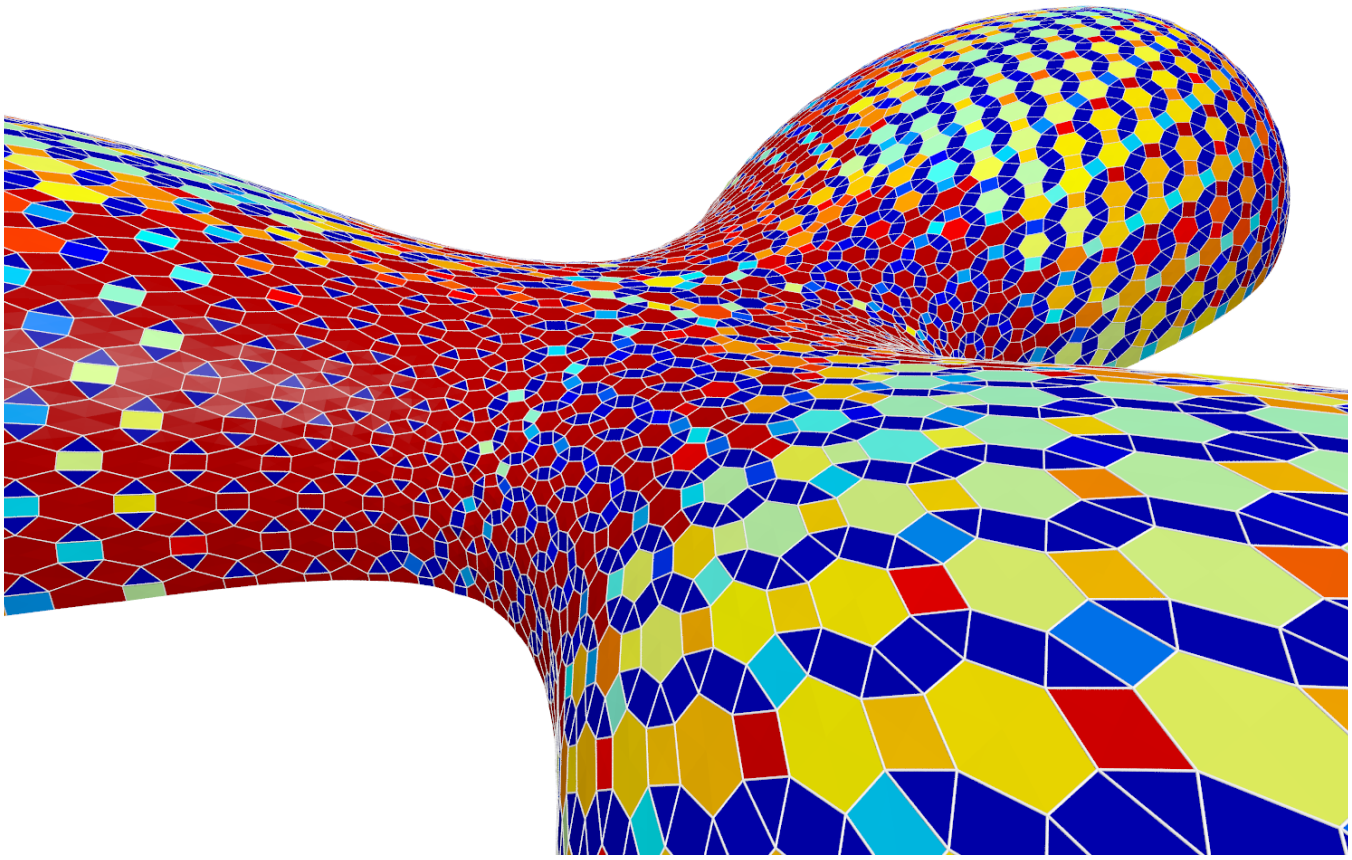

Figure 34: *The initial* $(4, 8, 8)$ *pattern shown in Figure 33 is not planar.*

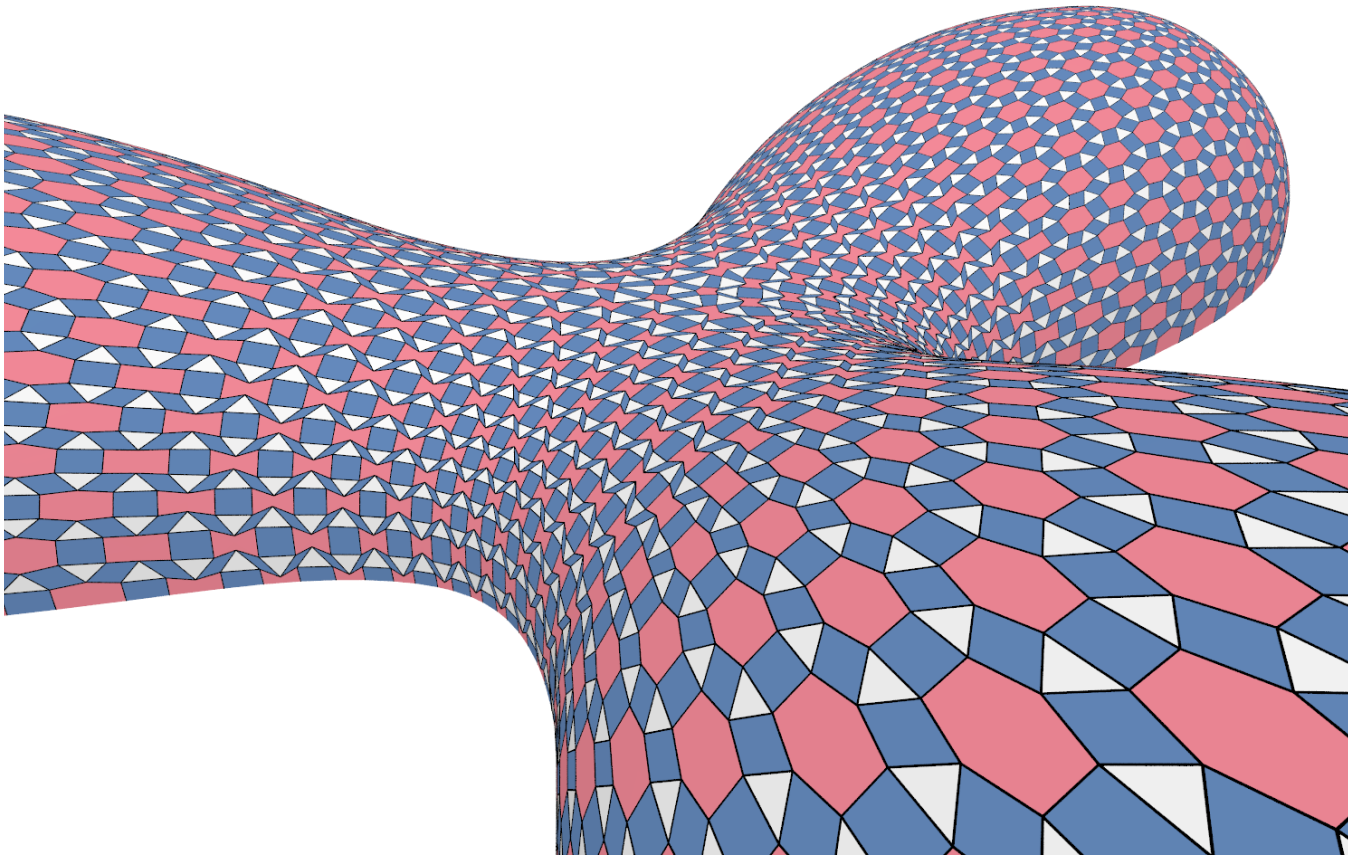

Figure 35: *An optimized polyheral pattern based on the initial pattern shown in Figure 33.*

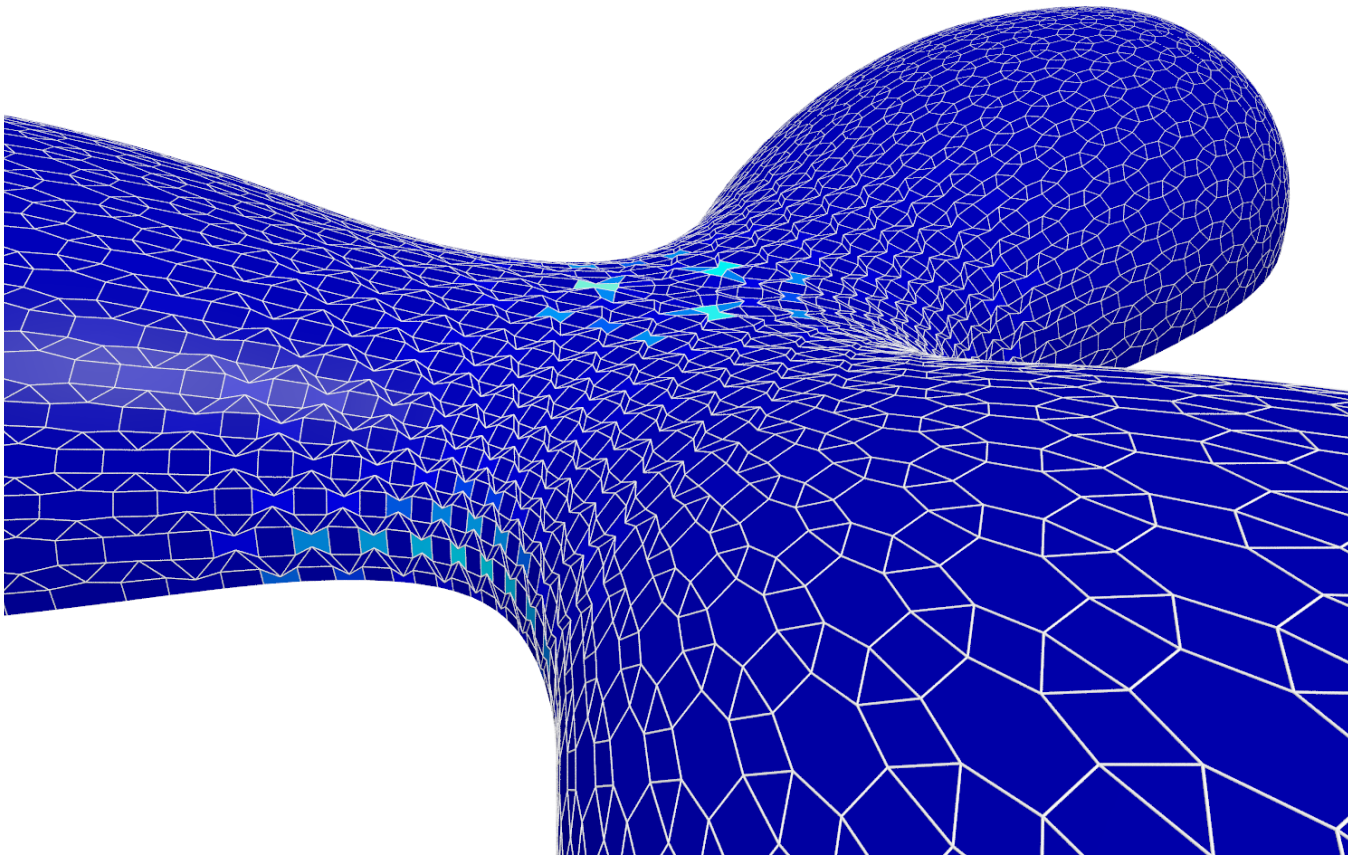

Figure 36: *The optimized pattern shown in Figure 35 is successfully planarized.*

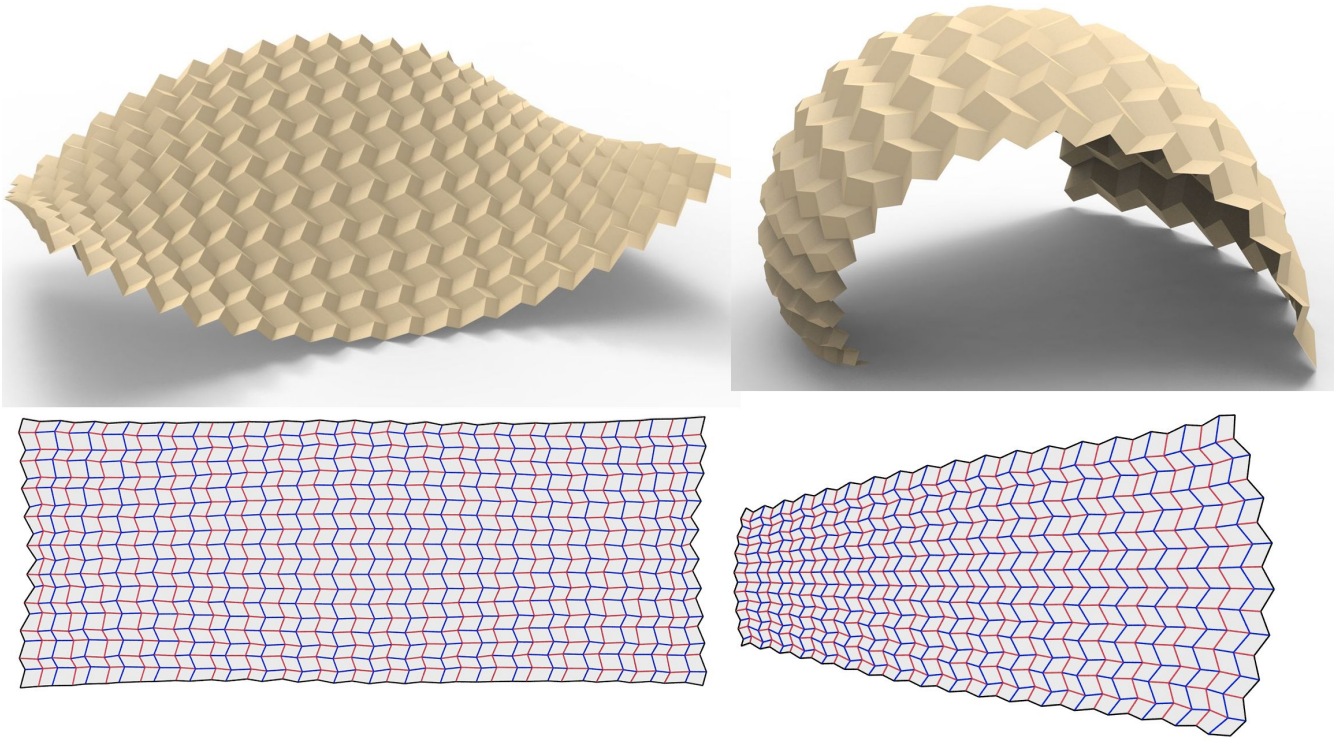

Figure 37: *An example of a Miura origami pattern. Such a pattern can be achieved using additional constraints in the optimization. We would like to explore the interactive design of such folding patterns in future work.*